

AL/EQ-TP-1996-0044

**UNITED STATES AIR FORCE
ARMSTRONG LABORATORY**



**Advanced Demilitarization Technology-
Disposal System for Laboratory
Quantities of Waste Material**

David S. Ross
Indira S. Jayaweera
Minggong Su
David Yao

SRI INTERNATIONAL
333 Ravenswood Avenue
Menlo Park, CA 94025-3493

May, 1996

19971215 062

DTIC QUALITY INSPECTED 3

Approved for public release; distribution is unlimited.

**Enviroics Directorate
Environmental Risk
Management Division
139 Barnes Drive, Suite 2
Tyndall Air Force Base FL
32403-5323**

NOTICES

This report was prepared as an account of work sponsored by an agency of the United States Government. Neither the United States Government nor any Agency thereof, nor any employees, nor any of their contractors, subcontractors, or their employees, make any warranty, expressed or implied, completeness, or usefulness of any privately owned rights. Reference herein to any specific commercial product, process, or service by trade name, trademark, manufacturer, or otherwise, does not necessarily constitute or imply its endorsement, recommendation, or favoring by the United States Government or any agency, contractor, or subcontractor thereof. The views and opinions of the authors expressed herein do not necessarily state or reflect those of the United States Government or any agency, contractor, or subcontractor thereof.


When Government drawings, specifications, or other data are used for any purpose other than in connection with a definitely Government-related procurement, the United States government incurs no responsibility or any obligation whatsoever. The fact that the Government may have formulated or in any way supplied the said drawings, specifications, or other data is not to be regarded by implication, or otherwise in any manner construed, as licensing the holder or any other person or corporation; or as conveying any rights or permission to manufacture, use, or sell any patented invention that may in any way be related thereto.

This technical report has been reviewed by the Public Affairs Office (PA) and is releasable to the National Technical Information Service (NTIS) where it will be available to the general public, including foreign nationals.

This report has been reviewed and is approved for publication.



JAMES A. HURLEY
Project Manager



ALLAN M. WEINER, LCol, USAF
Chief, Environmental Risk
Management

REPORT DOCUMENTATION PAGE

Form Approved
OMB No. 0704-0188

Public reporting burden for this collection of information is estimated to average 1 hour per response, including the time for reviewing instructions, searching existing data sources, gathering and maintaining the data needed, and completing and reviewing the collection of information. Send comments regarding this burden estimate or any other aspect of this collection of information, including suggestions for reducing this burden, to Washington Headquarters Services, Directorate for Information Operations and Reports, 1215 Jefferson Davis Highway, Suite 1204, Arlington, VA 22202-4302, and to the Office of Management and Budget, Paperwork Reduction Project (0704-0188), Washington, DC 20503.

1. AGENCY USE ONLY (Leave blank)		2. REPORT DATE 04 May 1996	3. REPORT TYPE AND DATES COVERED Final, 22 Feb 1994 - 1 May 1996	
4. TITLE AND SUBTITLE ADVANCED DEMILITARIZATION TECHNOLOGY - DISPOSAL SYSTEM FOR LAB QUANTITIES OF WASTE ENERGETIC MATERIAL			5. FUNDING NUMBERS PE: 63716D	
6. AUTHOR(S) David S. Ross, Indira S. Jayaweera, Minggong Su, and David Yao				
7. PERFORMING ORGANIZATION NAME(S) AND ADDRESS(ES) SRI International 333 Ravenswood Ave Menlo Park, CA 94025-3493			8. PERFORMING ORGANIZATION REPORT NUMBER	
9. SPONSORING/MONITORING AGENCY NAME(S) AND ADDRESS(ES) Armstrong Laboratory AL/EQM 139 Barnes Drive, Suite 2 Tyndall AFB, FL 32403			10. SPONSORING/MONITORING AGENCY REPORT NUMBER AL/EQ-TR-1996-0044	
11. SUPPLEMENTARY NOTES				
12a. DISTRIBUTION/AVAILABILITY STATEMENT Approved for public release; distribution is unlimited			12b. DISTRIBUTION CODE A	
13. ABSTRACT (Maximum 200 words) This is the final report of the disposal of laboratory quantities of energetic materials. SRI examined the use of very hot water as a medium for safe and complete disposal of energetic materials. The temperatures of the study were in the range of 200° - 350° C. One of the tasks dealt with the hydrothermolytic destruction of a range of pure energetic materials and various energetic formulations. The program found that the pure materials PETN, HBNQ, TNAZ, and TNT, and the formulations Pentolyte, Comp B, Octol, AFX-644, AFX-931, and PBXN-109 were all converted to simple inorganic ions and CO ₂ . Since AmP is water soluble, the ammonium nitrate work was conducted to develop some sense of the safe concentration limits in an aqueous system for hydrothermolytic destruction. The data obtained point to aqueous ammonium nitrate solutions that can be safely heated at concentrations up to about 12 wt %. AmP was found to be consumed at a rate apparently independent of starting pH. The products mirrored a widely ranging internal oxidation/reduction and included 40%, 15% and 15% of the starting nitrogen recovered respectively as N ₂ , N ₂ O and ammonium ion.				
14. SUBJECT TERMS hydrothermolytic destruction, PETN, HBNQ, TNAZ, TNT, Pentolyte, Tritonal, Comp B, Octol, AFX-644, AFX-931, PBXN-109			15. NUMBER OF PAGES 65	
			16. PRICE CODE	
17. SECURITY CLASSIFICATION OF REPORT Unclassified	18. SECURITY CLASSIFICATION OF THIS PAGE Unclassified	19. SECURITY CLASSIFICATION OF ABSTRACT Unclassified	20. LIMITATION OF ABSTRACT U	

PREFACE

This report was prepared by SRI International under contract F08635-94-C-0017, for the Armstrong Laboratory Environics Directorate (AL/EQ), Suite 2, 139 Barnes Drive, Tyndall Air Force Base, Florida 32403-5319.

This report describes the Disposal for Lab Quantities of Waste Energetic Material Project. This is the final report of the disposal of laboratory quantities of energetic materials. SRI examined the use of very hot water as a medium for safe and complete disposal of energetic materials. The temperatures of the study were in the range of 200° - 350° C. One of the tasks dealt with the hydrothermolytic destruction of a range of pure energetic materials and various energetic formulations. The program found that the pure materials PETN, HBNQ, TNAZ, and TNT, and the formulations Pentolyte, Comp B, Octol, AFX-644, AFX-931, and PBXN-109 were all converted to simple inorganic ions and CO₂. Since AmP is water soluble, the ammonium nitrate work was conducted to develop some sense of the safe concentration limits in an aqueous system for hydrothermolytic destruction.

The project was initiated under Captain William Gooden and completed under Mr. James A. Hurley of AL/EQM at Tyndall AFB, Florida.

DIC QUALITY INSPECTED

EXECUTIVE SUMMARY

In an earlier AF-sponsored program, SRI established that liquid water in the range 200°-350°C was an effective medium for the safe destruction of energetic materials (EMs) (Ross et al., 1993). The process took advantage of the fact that the materials are innately unstable and that their energetic nature is derived from oxidizing functionalities such as nitro and nitrate ester groups. The materials accordingly are structured to decompose energetically to simple, stable products such as CO₂ and, NH₃, N₂, although the ideal compositional balance is not present in many cases.

The safety of such a disposal process is derived from an expected difference in the disposition of the exoergic chemistry initiated when EMs are heated. Under normal heating conditions, the energy of such reactions would lead to internal heating of the bulk material, which in turn would lead autoignition and an energetic event. Under hydrothermal conditions, however, we expected that dissolution of the EM in the medium and rapid reaction at the water/EM interface would lessen the quantity of the bulk material at a rate greater than that for internal heating. An inherent safety factor was thus expected to be present in such systems.

Our study was oriented toward development of practical understanding of the hydrothermal destruction process. Accordingly it dealt with heterogeneous suspensions of both pure material, and formulations containing various combinations of materials.

The program was structured in two tasks. The first, the Core Program, dealt with the hydrothermolytic destruction of a range of pure EMs and various energetic formulations. The second task undertook a careful kinetics and product study of the destruction of ammonium picrate (Explosive D, AmP). That task was preceded by a brief study of the hydrothermolysis of ammonium nitrate, the results of which will also be discussed.

During the program, a patent was issued, titled Environmentally Acceptable Waste Disposal by Conversion of Hydrothermally Labile Compounds (US Patent No. 5,409,617). It covered our discovery of the accelerating effects of simple borate, silicate, and phosphate salts on EM hydrothermolysis; much of the work discussed in the patent was conducted under the earlier contract (Ross et al., 1993). Recently US patent application serial number 08/582,982 was filed as a continuation in part to the earlier patent to include the effects of sodium nitrite, discovered during this contract and described below.

TABLE OF CONTENTS

EXECUTIVE SUMMARY	v
I. INTRODUCTION	1
OBJECTIVE.....	1
BACKGROUND	1
SCOPE	1
APPROACH.....	1
II. CORE PROGRAM	3
EXPERIMENTAL PROCEDURES	4
Kinetic Studies.....	4
Products and Mass Balances.....	4
RESULTS	5
Pentaerythrotol tetranitrite (PETN)	5
HBNQ and TNAZ.....	9
TNT.....	11
Pentolyte.....	14
Tritonal.....	16
Comp B	17
Octol.....	19
AFX-644, AFX-931, and PBNX-109	20
III. AMMONIUM NITRATE	23
BACKGROUND	23
EXPERIMENTAL PROCEDURES	24
RESULTS AND DISCUSSION	24
IV. AMMONIUM PICRATE	27
BACKGROUND	27
EXPERIMENTAL PROCEDURES	28
Spectrophotometry.....	28
Product Studies.....	30
RESULTS.....	31
Kinetic Studies.....	31
Product Studies.....	34
DISCUSSION.....	36
V. CONCLUSIONS AND RECOMMENDATIONS	41
A PROPOSED NEW APPROACH.....	41
A PROPOSED NEW TECHNOLOGY	42
Background	42
Recent Supporting Data	45
SUMMARY AND PROPOSED ACTION.....	49
REFERENCES	51

LIST OF FIGURES

Figure 1. Kinetics studies of hydrothermolysis of PETN.....	6
Figure 2. Temperature dependence of the hydrothermolysis of PETN	6
Figure 3. Stable conversion products from the oxidation of organic materials.....	8
Figure 4. Hydrothermolyses of HBNQ and TNAZ at 200°C.....	9
Figure 5. Decomposition of a 1 wt% TNT at 300°C.....	12
Figure 6. Decomposition of Pentolyte.....	15
Figure 7. Comparison between the rates of hydrothermolysis of TNT alone and TNT in Pentolyte, Comp B, and Octol.....	15
Figure 8. The hydrothermolysis of TNT in Comp B at 300°C.....	18
Figure 9. The disappearance of TNT in Octol hydrothermolysis at 180°C and 210°C.....	20
Figure 10. Second-order plot for the loss of nitrate in the hydrothermolysis of ammonium nitrate	25
Figure 11. Spectrophotometric cell for kinetics studies in hydrothermal media	28
Figure 12. Spectrophotometric monitoring of the decomposition of TNT and AmP	30
Figure 13. Plot of half-life vs temperature for the hydrothermolysis of AmP in neutral water	31
Figure 14. Effects of starting pH on the hydrothermolysis of TNT	32
Figure 15. Spectrophotometric monitoring of the decay in the picrate signal	33
Figure 16. Consumption of PA and formation of nitrite and acetate.....	35
Figure 17. Acetate/OH ⁻ ratio as a function of temperature.....	36
Figure 18. Hydrothermolytic decomposition of PA	38
Figure 19. Solubility of sodium chloride and sodium carbonate in liquid water	41
Figure 20. Concept sketch	42

LIST OF FIGURES (continued)

Figure 21. Process flow diagram for carbonate-assisted hydrothermal oxidation.....	44
Figure 22. Data from supercritical water oxidation studies on dichlorobenzene	45
Figure 23. Comparison of interior corrosion and failure of reactor for conventional SCWO and uncorroded reactor for assisted hydrothermal oxidation of DCB	46
Figure 24. Destruction of hexachlorobenzene at 380°C with sodium carbonate.....	47

LIST OF TABLES

Table 1. Core Program Materials	3
Table 2. Hydrolysis of PETN in Neutral Water	6
Table 3. Products from the Hydrothermolysis of PETN	7
Table 4. Products from the Exhaustive Hydrothermolysis of HBNQ	10
Table 5. Products from the Hydrothermolysis of TNAZ	11
Table 6. Product from the Hydrothermolysis of TNT and Sodium Nitrite.....	13
Table 7. Products from the Exhaustive Hydrothermolysis of Pentolyte.....	16
Table 8. Products from the Hydrothermolysis of Tritonal.....	17
Table 9. Products from the Hydrothermolysis of Comp B	19
Table 10. Products from the Hydrothermolysis of Octol.....	21
Table 11. Products from the Hydrothermolysis of AFX-644.....	21
Table 12. Products from the Hydrothermolysis of AFX-931.....	22
Table 13. Products from the Hydrothermolysis of PBXN-109.....	22
Table 14. Products from the Exhaustive Destruction of PA.....	34

I. Introduction

Objective

This program was undertaken to determine the effectiveness of hydrothermal destruction on candidate energetic waste materials

Background

The process took advantage of the fact that the materials are innately unstable and that their energetic nature is derived from oxidizing functionalities such as nitro and nitrate ester group. The materials are accordingly structured to decompose energetically to simple, stable products such as CO_2 and NH_3 , N_2 although the ideal compositional balance is not present in many cases.

Scope

The study was oriented toward development of practical understanding of the hydrothermal destruction process. Accordingly it dealt with heterogeneous suspensions of both pure material, and formulations containing various combinations of materials.

Approach

The program was structured in two tasks. The first, the Core Program, dealt with the hydrothermal destruction of a range of pure EMs and various energetic formulations. The second task undertook a careful kinetics and product study of the destruction of ammonium picrate (Explosive D, AmP). That task was preceded by a brief study of the hydrothermolysis of ammonium nitrate.

II. CORE PROGRAM

This portion of our program was undertaken to determine the effectiveness of hydrothermal destruction on candidate energetic waste materials. The list of candidates established during a visit to SRI on 22 February 1994 by Captain William Gooden is presented in Table 1. Some of the materials were supplied by the Air Force; others were available to us from SRI's EM depository.

Table 1. Core Program Materials

EM	Formula/Composition	Source
PETN	Pentaerythritol tetranitrate	SRI
HBNQ	High bulk nitroguanidine	SRI
TNAZ	1,3,3-Trinitroazetidine	Air Force
TNT	2,4,6-Trinitrotoluene	SRI
Pentolyte	50% TNT, 50% PETN	Air Force
Tritonal	80% TNT, 20% Al	Air Force
Comp B	60% RDX, 40% TNT, 1% wax	Air Force
Octol	75% HMX, 25% TNT	Air Force
AFX-644	40% NTO, 30% TNT, 20% 1401 Al, 9.85% I-800 wax, 0.15% ganex wax	Air Force
AFX-931	37% AP, 32% RDX, 15% Al, 7.26% R45HT, 7.26% DOA, 1.12% IDPI, 0.26% DHE, 0.0015% FeAA, 0.1% antioxidant	Air Force
PBXN-109	63.5% RDX, 20% Al, 7.5% R45-HT, 7.5% DOA, 1.1% IDPI, 0.0015% FeAA, 0.26% DHE, 0.1% antioxidant	Air Force

In most cases the studies included both kinetics studies of the decompositions of these materials and determinations of the products from exhaustive destruction.

EXPERIMENTAL PROCEDURES

Kinetic Studies

Both stainless steel and quartz batch reactors, 5 mL in volume, were used. The former were constructed of 316 stainless steel tubes (0.25-inch OD, 0.035-inch wall thickness) sealed with Swagelok end caps. Since the EMs were insoluble in water, stock solutions were prepared by dissolving known quantities in acetone. The acetone was then removed with a helium stream. Deionized water (4mL) was added, and the reactors were sealed, the steel reactors with end caps and the quartz reactors heat sealed with a torch. In the quartz cases, care was taken not to heat the solution as the tube was being heated. Manipulations were performed under He to ensure that no atmospheric oxygen entered the reactors.

The reactors were then heated in a thermostated oven set to the target temperature. When the quartz reactors were heated to temperatures greater than 250°C, they were placed into small steel bombs containing enough waste to provide a pressure balance at temperature.

They were removed from the oven sequentially and quenched in ice. The reaction progress was monitored by analyzing for remaining EM. The analyses were conducted on Hewlett Packard 1050 or 1090 high pressure liquid chromatographs, using an ODS Hypersil, 5- μ m, 200 x 4.6 mm column. The temperature was 40°C and the mobile phase was 50:50 acetonitrile:water.

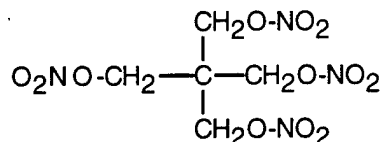
Products and Mass Balances

Experiments were conducted in 28-30 mL stainless steel autoclaves lined with quartz tubes. Each autoclave containing 10 mL of deionized water was loaded with 100-200 mg of EM. When the effect of salt was studied, appropriate quantities of salt were added to the water. The autoclaves were then pressurized with helium to 70 psi and heated in a thermostated oven at a predetermined temperature.

After the treatment, gas products were sampled through the reactor valve and analyzed using a Hewlett Packard gas chromatograph. The liquid products were analyzed using a Dionex 2000i ion chromatograph and a Hewlett Packard 1050 or 1090 liquid chromatograph. When residues were found, elemental analyses for C, N, and H were performed on the residues with a Perkin-Elmer 2400 elemental analyzer.

RESULTS

Pentaerythrotetranitrite (PETN)



PETN

PETN is a waxy solid melting at 141°C. Its thermal decomposition has been studied by many workers, but there is no general agreement about the decomposition mechanism or the values of its Arrhenius parameters. In an account of extensive work, Roth concluded that the decomposition is a very complex reaction series that includes autocatalytic and autoretarding processes (Roth, 1950).

Kinetics Studies. The decomposition of PETN was studied with 0.25% slurries in neutral water at 145°, 160°, 175°, and 190°C; a run with 0.1 M KOH was also conducted at 160°C. The consumption was not first order and is best viewed as a zero-order process as shown in Figure 1. The zero-order plots are reasonably well fit with the lines shown, and the regression coefficients presented in Table 2 are satisfactory. Lines in such plots should ideally pass through the origin, and the off-sets in the figure are probably due to temperature accommodation at the start of each run.

Table 2 also presents the rate constants derived from Figure 1. A zero-order process is confirmed by the fact that the addition of 0.1 M KOH had essentially no effect on the rate, in the face of the known base catalyzed decomposition of nitrate esters (Capellos et al., 1984). Figure 2 presents the temperature dependence of the hydrothermolysis in graphical form.

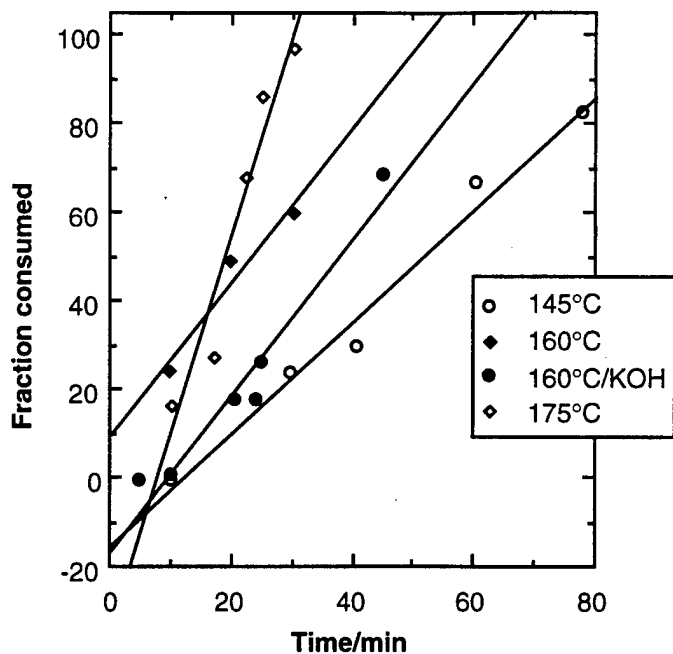


Figure 1. Kinetic studies of hydrothermolysis of PETN in neutral water and in KOH. The 190°C data have been omitted for clarity.

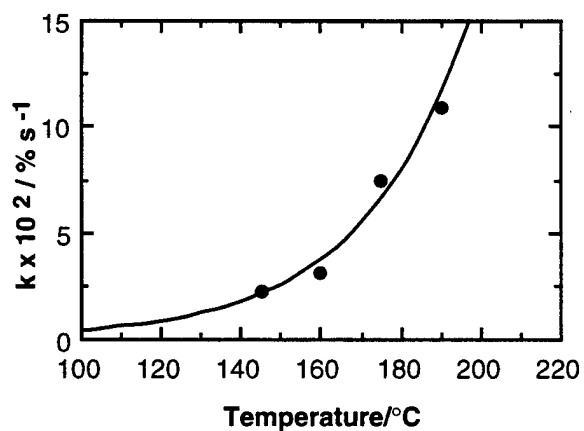


Figure 2. Temperature dependence of the hydrothermolysis of PETN in unagitated runs.

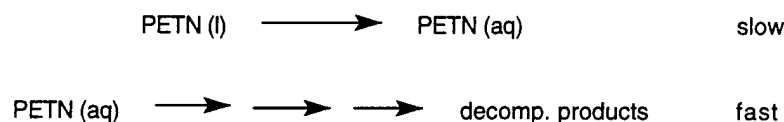
Table 2. Hydrolysis of PETN in Neutral Water and in Aqueous KOH

Temperature (°C)	R ² a	k/% s ⁻¹ (x 10 ²)
145	0.980	2.2
160	0.965	3.1
160 ^b	0.965	3.0
175	0.935	7.5
190	0.905	10.9

a. Regression coefficient.

b. In 0.1 M KOH.

In this heterogeneous system, the overall process appears to be governed by a slow dissolution of PETN into the aqueous phase, followed by rapid hydrolysis and decomposition.



Agitation should, of course, substantially increase the rate of destruction.

Products and Mass Balance. Product analyses were conducted on resulting mixtures from exhaustive decompositions at 200°C/30 min. The gas phase products were N₂O, N₂, CO, and CO₂, and NO₂⁻, NO₃⁻, NH₄⁺, CH₃CO₂⁻ and were the ionic products found in the recovered aqueous phase. The data are presented in Table 3.

Table 3. Products from the Hydrothermolysis of PETN at 200°C/30 min^a

Phase	Product	Fraction of Starting C/N (%) ^b
Nitrogen		
Product gases	N ₂ O	24
	N ₂	8
Products in solution	nitrite	1
	nitrate	46
	ammonium	5
Total N accounted for		84
Carbon		
Product gases	CO ₂	24
	CO	14
Products in solution	formate	12
	acetate	18
	glycolate	.c
	oxalate	.c
Total C accounted for		68

a. Exhaustive destruction.

b. Reported as final yields in percent of initial carbon and nitrogen.

c. Found at trace levels.

Table 3 shows that 68% and 84%, respectively, of the starting C and N were accounted for, although we expect that most of the unaccounted for carbon was present as bicarbonate. We observed no other carbon fragments, but underscore the point that the relatively mild conditions resulted in the cleavage of most of the C-C bonds.

Acetate was initially a surprising product since there are no methyl groups in the starting PETN. We soon recognized, however, that its formation, along with that of oxalate, bicarbonate, and other very stable products, is to be expected if thermodynamics drives the process. Figure 3 presents the free energies of formation of several products expected from such a scenario, and as we shall see below in the hydrothermolytic destruction of other energetic materials, their presence in product mixtures reflects thermodynamic control, which in turn must be driving an elaborate and energetic decomposition sequence. That likelihood is confirmed by the recovered nitrogen species, which include N_2O , N_2 , and ammonium ion, all highly reduced with respect to the starting nitro groups. The entire process must be one in which extensive electron transfer accompanies a cascade of intermediates, culminating in thermodynamically favored products.

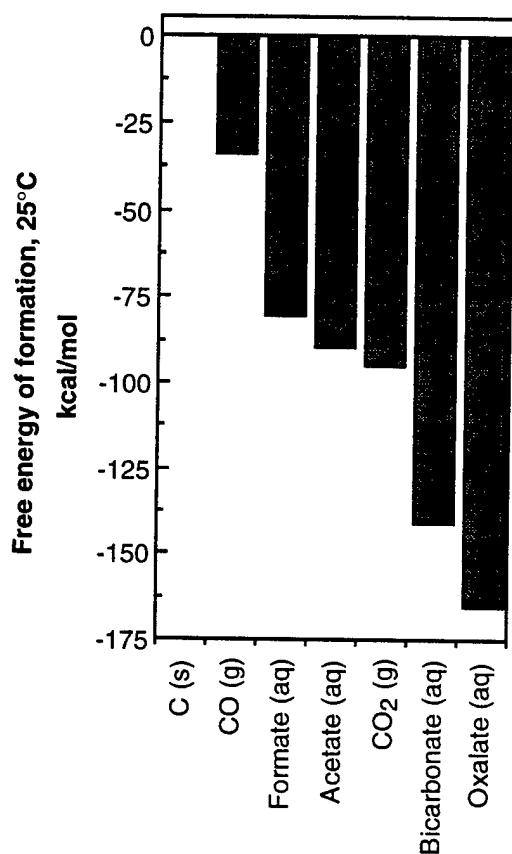
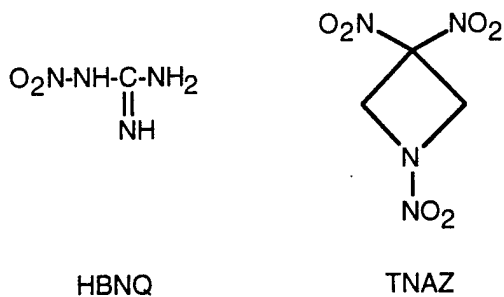


Figure 3. Stable conversion products from the oxidation of organic materials (from Latimer, 1952).

HBNQ (High Bulk Nitroguanidine) and TNAZ (1,3,3-Trinitroazetodine)



HBNQ and TNAZ are both white crystalline solids, melting, respectively, at 232°C and 101°C. The TNAZ low melting point makes it useful as an oxidizer in cast or melt explosives. Because these compounds were expected to hydrolyze quickly, we conducted only brief, semiquantitative kinetics studies and focused on identifying the hydrothermolytic products.

Kinetics Study. The hydrothermolyses were studied at 200°C in neutral water, and the results are shown in Figure 4. The data for HBNQ and TNAZ are consistent, respectively, with a first-order hydrolysis having a rate constant of about $3.9 \times 10^{-3} \text{ s}^{-1}$ and a zero-order hydrolysis having a rate constant of about $5.0 \times 10^{-2} \% \text{ s}^{-1}$. These modes of loss are not surprising based on an anticipated satisfactory solubility of HBNQ in water, while TNAZ is likely highly insoluble in water. Thus, like PETN, the rate of destruction of TNAZ depends on the rate of dissolution.

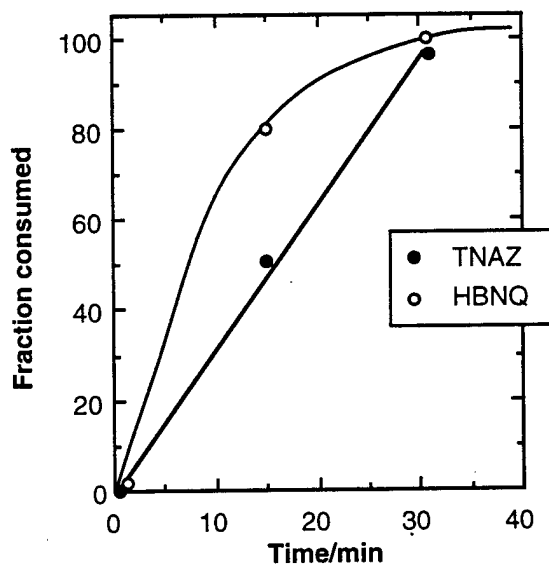


Figure 4. Hydrothermolyses of HBNQ and TNAZ at 200°C.

Product and Mass Balances. The solution and gas phase hydrothermolytic decomposition products from the exhaustive destructions of HBNQ and TNAZ at 300°C were determined, and the observed carbon and nitrogen balances are shown in Tables 4 and 5. Table 4 shows that we can account for virtually all the starting nitrogen and carbon in HBNQ, with the data reflecting simple exhaustive hydrolysis having the stoichiometry



Table 4. Products from the Exhaustive Hydrothermolysis of HBNQ at 300°C/240 min^a

Phase	Product	Fraction of Starting C/N (%) ^b
Nitrogen		
Product gases	N ₂ O	30
	N ₂	4
Products in solution	Nitrite	--c
	Nitrate	--c
	Ammonium	64
	Total N accounted for	97
Carbon		
Product gases	CO ₂	100
	CO	--c
Product solution	Formate	--c
	Total C accounted for	100

- a. Trace quantities of HBNQ were recovered at levels estimated to be 0.1% of the starting quantity.
 b. Reported as final yields in percent of initial carbon and nitrogen.
 c. Found at trace levels.

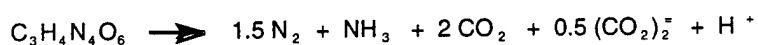
For the TNAZ case in Table 5, we can account for close to 90% of the starting nitrogen and about 95% of the starting carbon. In this, case clearly more than hydrolysis takes place, with virtually all the carbon oxidized to CO₂ and oxalate. Once again we see evidence of an essentially

Table 5. Products from the Hydrothermolysis of TNAZ at 300°C/240 min

Phase	Product	Fraction of Starting C/N (%) ^a	
Nitrogen	Product gases	N ₂ O	21
		N ₂	55
	Product solution	Nitrite	..b
		Nitrate	..b
		Ammonium	13
Total N accounted for		89	
Carbon	Product gases	CO ₂	52
		CO	3
	Product solution	Formate	..b
		Acetate	1
		Oxalate	39
		Total C accounted for	

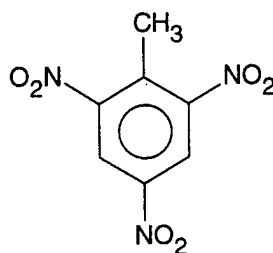
a. Reported as final yields in percent of initial carbon and nitrogen.
 b. Found at trace levels.

complete oxidation-reduction sequence to thermodynamically -favored products. The entire stoichiometry is difficult to model; however,



is probably a fair reflection of the process.

TNT (2,4,6-Trinitrotoluene)



TNT

TNT (mp 82°C) is an easily synthesized, inexpensive, common explosive. It is used in a number of formulations, many of which have been studied in this program as described below. In our earlier AF program (Ross et al., 1993), we demonstrated that TNT could be effectively

destroyed under hydrothermal conditions and that the process can be catalyzed by silicate and borate salts (Ross et al., 1995). That earlier study, however, was conducted with TNT/water solutions, whereas the practical destruction of TNT-bearing waste would involve considerably larger quantities slurried in water. The work here was conducted with TNT/water slurries containing up to 1% TNT.

The added silicates and borates substantially enhance the decomposition rate of TNT, but the formation of carbonaceous residue was inevitable under a range of conditions. The major work conducted in this portion of the program was to examine the effects of added nitrite, which fully eliminated the residue, and increased the rate of destruction.

Kinetic Study. Decomposition of TNT at 300°C in water was conducted with and without added sodium nitrite in 5-mL stainless steel reactors containing a slurry of 30 mg of TNT in 3 mL of water. For the nitrite-added runs, 91 mg of sodium nitrite was added to the reactors. The results are compared in Figure 5.

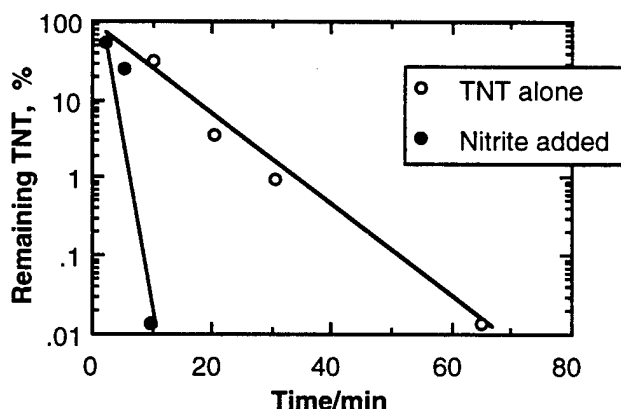


Figure 5. Decomposition of a 1 wt% TNT at 300°C. The molar ratio of nitrite to TNT is 10 to 1.

Figure 5 shows that TNT decomposes in a first-order process; unlike PETN, it must therefore dissolve readily before hydrothermolysis. Figure 5 also shows that the added nitrite accelerated the loss rate for TNT. The values of the first order rate constants developed from the plot are $2.4 \times 10^{-3} \text{ s}^{-1}$ and $1.9 \times 10^{-2} \text{ s}^{-1}$ for the TNT alone and TNT with nitrite added, respectively, or almost an order of magnitude increase in rate.

Products and Mass Balances. Decomposition of TNT at 300°C in water was conducted both with and without added sodium nitrite. The product data are presented in Table 6,

which also includes the decomposition data for sodium nitrite alone in water under the same conditions.

As mentioned above, the decomposition of TNT alone in water yielded a dark residue corresponding to about 45% of the starting mass of the TNT, that contained sizable quantities of both carbon and nitrogen. The major gases and soluble products were CO₂, CO, N₂O, N₂, and ammonium ion.

The addition of sodium nitrite strikingly eliminated the organic residue and clearly increased the conversion of carbon to CO₂/bicarbonate by a factor greater than 4. Table 6 shows that sodium nitrite itself is essentially stable under the conditions, and the consumption of nitrite in the run with TNT reflects some manner of stoichiometric reaction, rather than a catalyzed conversion.

Table 6. Product from the Hydrothermolysis of TNT and Sodium Nitrite at 300°C/120 min^a

Phase	Product	Fraction of Starting C/N (%) ^b		
		TNT alone	TNT and 3% NaNO ₂	3% NaNO ₂ alone
Carbon Gas	CO ₂	17	13	-
	CO	1	.c	-
	CH ₄	.d	.c	-
Solution	Acetate	4	11	-
	Formate	.d	.c	-
	Glycolate	.d	1	-
	Oxalate	.d	.c	-
	Bicarbonate	.d	61	-
Recovered solid	-	62	None ^d	-
Total C accounted for		84	85	-
Nitrogen Gas	N ₂ O	.c	14	.c
	N ₂	30	28	2
Solution	Nitrite	.c	35	90
	Nitrate	.c	2	1
	Ammonium	28	8	.c
Recovered solid	-	31	none ^d	
Total N accounted for		89	87	93

a. Full conversion.

b. Reported as final yields in percent of initial carbon and nitrogen.

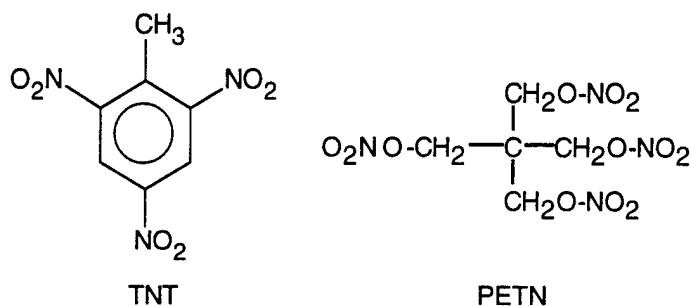
c. Trace quantities recovered.

d. A small quantity of a white solid was recovered and is likely silica derived from the quartz liner of the reactor.

While this result is meaningful and potentially useful, the nitrite/TNT ratio of about 10/1 and the consumption of 65% of the nitrite could be limitations to the practicality of the process. Further development would require studies to establish values for the least quantities of nitrite necessary for satisfactory conversion.

Pentolyte

Pentolyte is a castable 50/50 mixture of TNT and PETN and has been used in hand and antitank grenades.



Kinetic Study. Comparison of Figures 2 and 5, which display the hydrothermolysis rates for PETN and TNT, respectively, shows that PETN is considerably less stable than TNT under hydrothermolytic conditions. Thus, while the two materials respectively decompose in zero-order and first-order manners, the initial decomposition rate of TNT of about 0.2% s⁻¹ at 300°C is matched by that for PETN at about 200°C. Accordingly, the pentolyte destruction was followed by the loss of TNT.

The rate of destruction was measured at 210° and 230°C, and Figure 6 shows the results in a first-order plot. The first-order rate constants at the two temperatures are 1.5 x 10⁻⁴ s⁻¹ and 4.4 x 10⁻⁴ s⁻¹ respectively. Figure 7 shows the satisfactory agreement with these data and those for TNT alone (Ross et al., 1993) as well as data for other TNT-containing formulations discussed below.

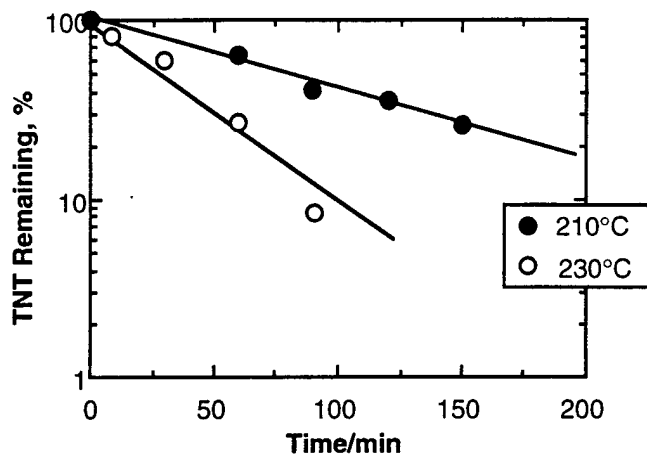


Figure 6. Decomposition of Pentolyte (50 μM) at 210° and 230°C.

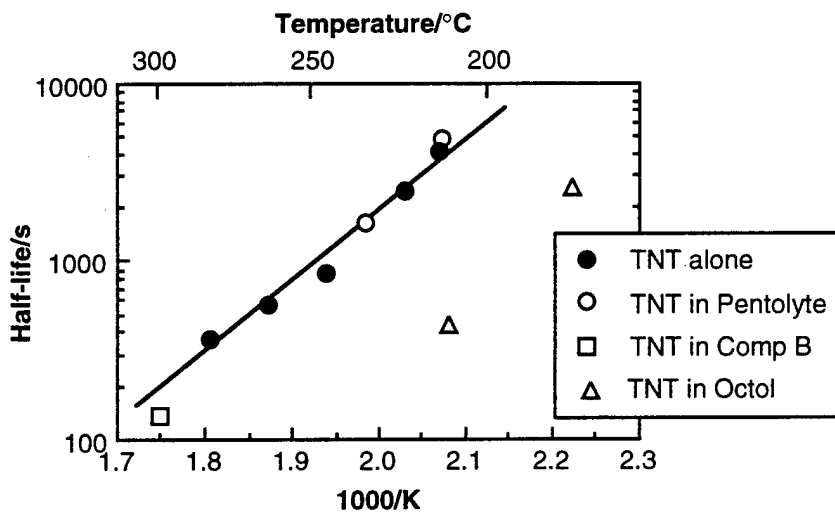


Figure 7. Comparison between the rates of hydrothermolysis of TNT alone and TNT in Pentolyte, Comp B, and Octol.

Products and Mass Balance. Table 7 shows the products of the exhaustive decomposition of pentolyte at 300°C and accounts for better than 80% of the starting carbon and nitrogen. As expected for a material containing TNT, about half the starting carbon and a smaller fraction of the starting nitrogen are converted to a filterable solid; the remaining identified C and N are recovered essentially as oxalic and formic acids and ammonium nitrate. The missing carbon is probably in the recovered aqueous phase as bicarbonate.

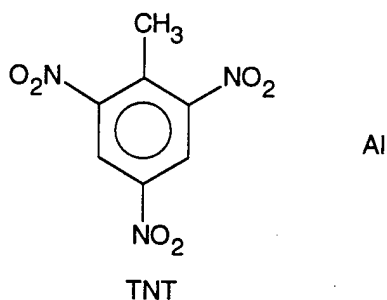
Table 7. Products from the Exhaustive Hydrothermolysis of Pentolyte at 300°C/60 min

Phase	Product	Fraction of Starting C/N (%) ^a	
Carbon			
	Gas	CO ₂ CO	5 .b
Solution	Oxylate Formate	12 12	
	Recovered solid	-	52
Total C accounted for		81	
Nitrogen			
	Gas ^b Solution	N ₂ O	1
Solution	Nitrite Nitrate Ammonium	3 30 32	
	Recovered solid	-	18
	Total N accounted for		84

a. Reported as final yields in percent of initial carbon and nitrogen.
b. Found at trace levels.

Tritonal

Tritonal is an 80% TNT, 20% Al mixture. It is a castable explosive sometimes used for underwater applications.



Only product data were obtained in this case, and the experiments were conducted in 30-mL stainless steel reactors on 1% slurries in water.

Table 8 shows the product data for exhaustive tritonal hydrothermolysis at 300°C. We can account for better than 90% of the starting carbon and nitrogen. Once again, we find that a material containing TNT yields a residue.

Table 8. Products from the Hydrothermolysis of Tritonal at 300°C/240 min

Phase	Product	Fraction of Starting C/N (%) ^a
Carbon		
Gas	CO ₂	46
	CO	2
Solution	Acetate	2
	Formate	2
Recovered solid	-	47
Total C accounted for		99
Nitrogen		
Gas ^b	N ₂ O	nd
	N ₂	24
Solution	Nitrite	.b
	Nitrate	.b
	Ammonium	45
Recovered solid	-	22
Total N accounted for		91

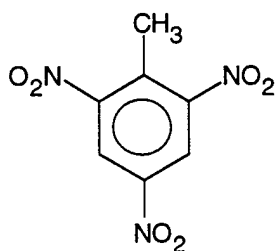
a. Reported as final yields in percent of initial carbon and nitrogen.

b. Found at trace levels.

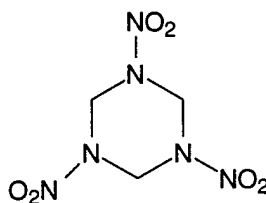
Comparison with the data in Table 6 for pure TNT shows that presence of aluminum affects the conversion substantially. Thus in that case 17% and 28% of the starting carbon and nitrogen, respectively, were recovered as carbon dioxide and ammonium. In the tritonal case the values, respectively, are 46% and 45%. Aluminum appears to drive the hydrothermolysis further along to the thermodynamically favored products.

Comp B

Comp B is a mixture of RDX and TNT, commonly in a 3/2 ratio, although other compositions have been used. It is a very common explosive, used in bombs, bursting charges, and antisubmarine activity. It was studied here in 1% slurries in water.



TNT



RDX

Kinetic Study. As for pentolyte, the TNT is the less reactive component of the formulation, and the Comp B decomposition was monitored in terms of the TNT hydrothermolysis. The results at 300°C are shown in Figure 8. It appears that the TNT loss is best represented by the S-shaped curve in the figure, reflecting an accelerating hydrothermolysis following an induction period. Although initially unexpected, in retrospect the behavior can be anticipated since nitrite is a major RDX hydrothermolysis product, is produced in minutes at 300°C (Ross et al., 1993), and in turn nitrite promotes TNT hydrothermolysis as discussed above. Thus the relatively rapidly decomposing RDX promotes the decomposition of the TNT.

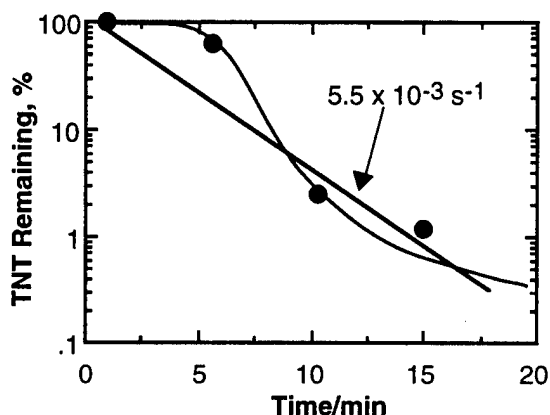


Figure 8. The hydrothermolysis of TNT in Comp B at 300°C. The sigmoid curve best fits the data; the first-order line is for a rough comparison with data for neat TNT.

Also shown in Figure 8 is a line roughly in accord with a first-order disappearance for comparison with data for the hydrothermolysis of pure TNT. That comparison is made in Figure 7, which shows that in the present case, the overall TNT decomposition is modestly accelerated.

Products and Mass Balance. Since the presence of TNT in the formulation suggested the formation of a residue, the program included experiments with added nitrite. The results are presented in Table 9. In the case of Comp B alone, about 48% of starting carbon and 8% of nitrogen were recovered as a dark residue. Thus the nitrite from the RDX decomposition is not in sufficient quantity to eliminate the residue. (The missing carbon is likely present as bicarbonate.) In contrast, in the sodium nitrite-added work we find the residue to be fully eliminated, and the carbon is essentially fully oxidized to carbon dioxide and bicarbonate. Both carbon and nitrogen recoveries are satisfactory.

Table 9. Products from the Hydrothermolysis of Comp B at 300°C/240 min

Phase	Product	Fraction of Starting C/N (%) ^a		
		Comp B alone 300°C/240 min	Comp B with 3% NaNO ₂ 300°C/60 min	
Carbon	Gas	CO ₂	16	26
		CO	1	.b
Solution		Acetate	3	.b
		Glycolate	3	.b
		Oxalate	2	.b
		Formate	1	.b
		Carbonate	.c	66
		Recovered solid	-	48
Total C accounted for		74	92	
Nitrogen	Gas ^b	N ₂ O	10	38
		N ₂	42	25
Solution		Nitrite	.c	31
		Nitrate	1	6
		Ammonium	16	4
		Recovered solid	-	8
Total N accounted for		77	104	

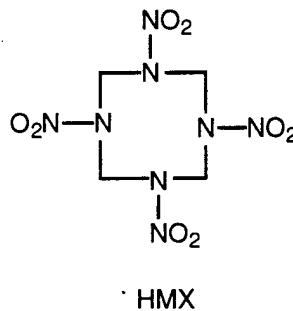
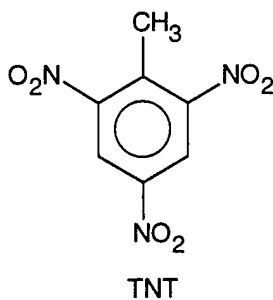
a. Reported as final yields in percent of initial carbon and nitrogen.

b. Found at trace levels.

c. Not measured.

Octol

Octols are HMX/TNT mixtures, commonly in a 75/25 ratio. They are used in fragmentation and shaped charge applications as well as formation fracturing agents in oil exploration.



Kinetic Study. Kinetic runs were conducted at 180° and 210°C; the results are shown in a first-order plot in Figure 9. The first-order rate constants developed from these data are $2.5 \times 10^{-4} \text{ s}^{-1}$ and $1.5 \times 10^{-3} \text{ s}^{-1}$, respectively.

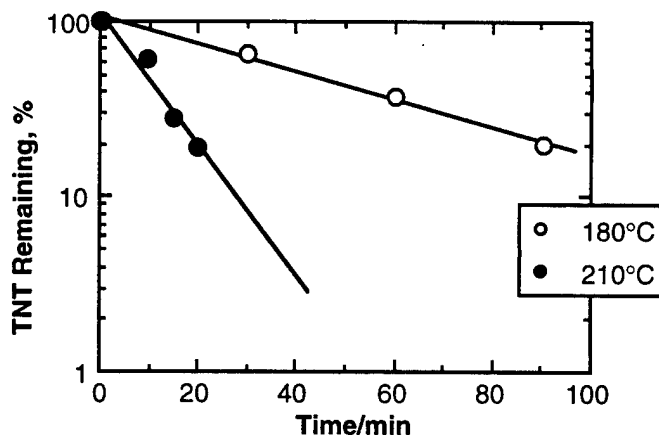


Figure 9. The disappearance of TNT in octol hydrothermolysis at 180° and 210°C.

Given the similar hydrothermolysis chemistry for RDX and HMX (Ross et al., 1993), we would expect octol and Comp B to behave similarly. There is, however, a considerable difference. Thus the data in Figure 9 satisfactorily display a first-order disappearance, while those for Comp B in Figure 8 do not. The difference is continued in Figure 7, where the Octol-TNT disappearance is significantly promoted, unlike the Comp B case. The increase at 210°C is strikingly about an order of magnitude; thus the TNT loss rate at 210°C is comparable to the rate for TNT alone at 275°C. We have no specific explanation for these differences, but note that as for RDX, nitrite is a major decomposition product in HMX hydrothermolysis.

Product and Mass Balance. Table 10 presents the product data for exhaustive octol hydrothermolysis. As for Comp B, despite the nitrite production from the nitramine component, there is a significant residue. Curiously, in this case methyl amine is a significant product.

AFX-644, AFX-931, and PBXN-109

These three formulations were considered only briefly, with little need for kinetics study based on the data already accumulated for similar mixtures of the major components. The products of their exhaustive hydrothermolyses were determined and are listed in Tables 11, 12, and 13.

Table 10. Products from the Hydrothermolysis of Octol at 300°C/240 min

Phase	Product	Fraction of Starting C/N (%) ^a
Carbon		
Gas	CO ₂	26
	CO	.b
Solution	Acetate	2
	Formate	1
	CH ₃ NH ₂	5
Recovered solid	-	38
Total C accounted for		73
Nitrogen		
Gas ^b	N ₂ O	42
	N ₂	24
Solution	Nitrite	1
	Nitrate	1
	Ammonium	6
	CH ₃ NH ₂	5
Recovered solid	-	5
Total N accounted for		84

a. Reported as final yields in percent of initial carbon and nitrogen.

b. Found at trace levels.

Table 11. Products from the Hydrothermolysis of AFX-644 at 300°C/240 min

Phase	Product	Fraction of Starting C/N (%) ^a
Nitrogen		
Product gases	N ₂	52
Product solution	Nitrite	52
	Ammonium	.b
Recovered solid	-	10
Total N accounted for		114
Carbon		
Product gases	CO ₂	21
	CO	2
Product solution	Formate	2
	Acetate	10
Recovered solid	-	46
Total C accounted for		81

a. Reported as final yields in percent of initial carbon and nitrogen.

b. Found at trace levels.

Table 12. Products from the Hydrothermolysis of AFX-931 at 300°C/240 min

Phase	Product	Fraction of Starting C/N (%) ^a
Nitrogen		
Product gases	N ₂ O	25
	N ₂	30
Product solution	Nitrite	.b
	Nitrate	.b
	Ammonium	28
	Recovered solid	-
Total N accounted for		83
Carbon		
Product gases	CO ₂	13
	CO	4
Product solution	Formate	.b
	Acetate	1
	Oxalate	5
Recovered solid		27
Total C accounted for		51

a. Reported as final yields in percent of initial carbon and nitrogen.
b. Found at trace levels.

Table 13. Products from the Hydrothermolysis of PBXN-109 at 300°C/240 min

Phase	Product	Fraction of Starting C/N (%) ^a
Carbon		
Gas	CO ₂	33
	CO	1
Solution	Acetate	.b
	Formate	.b
Recovered solid		51
Total C accounted for		85
Nitrogen		
Gas	N ₂ O	19
	N ₂	33
Solution	Nitrite	12
	Nitrate	16
	Ammonium	12
Recovered solid		.b
Total N accounted for		91

a. Reported as final yields in percent of initial carbon and nitrogen.
b. Found at trace levels.

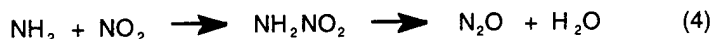
III. AMMONIUM NITRATE

BACKGROUND

Central to the safe use of very hot aqueous media in the disposal of energetic materials is the effect of the dissolution of water-soluble EMs on the thermally promoted reactions leading to autoignition. Specifically, we need to know the concentration limits in an aqueous system below which no autoignition can take place. Because dissolution should provide some degree of safety, we preceded the AmP work with a brief study of hydrothermolysis of ammonium nitrate (AN) at 350°C to measure its effect.

The basis of this approach is the work of Brower et al. (1989), who have described the decomposition of neat AN in the melt. In studies in the range 200°-365°C involving 1-4 mg samples in sealed tubes, they found that AN decomposed cleanly in a first-order manner. Their data suggested that an ionic decomposition dominated below 290°C .

At higher temperatures, appropriate to the present discussion, they found that the data supported a free radical decomposition route involving OH.



That sequence leads through nitramide (NH_2NO_2) to N_2O and H_2O , and we can expect that this exoergic chemistry leads the system ultimately to autoignition.

The decomposition kinetics of Brower et al. were satisfactorily obtained with no autoignition, a finding we suggest can be applied directly to matters of safety. Our extension of their data here is conducted with an understanding of its limitations, which include their small sample sizes and the fact that times to explosion for loosely held EMs depend somewhat on the geometry of the confinement. We have hoped, nonetheless, to develop some sense of the safety boundaries in hydrothermal EM solutions. Recognizing that autoignition develops if the rate of self-heating in a heated EM system is greater than the rate of heat dissipation, since the rate of self-

heating is related directly to reaction rate, we can use the characteristic times for reaction in the Brower et al. work to estimate a safe regime. Indeed, given the substantial heat capacity of water and that the self-heating of an aqueous EM solution should be significantly less than that for the neat material, the result of this exercise should be a lower limit value.

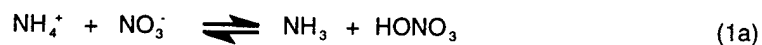
EXPERIMENTAL PROCEDURES

A stock solution of ammonium nitrate was prepared by dissolving a known amount of ammonium nitrate in water. Reactions were conducted in 30-mL autoclaves lined with quartz tubing; 10 mL of stock solution was transferred into each autoclave and dissolved air was by purging with He. Autoclaves were then sealed under He.

Autoclaves were heated in a thermostated oven heated to the required temperature. Samples were removed sequentially and quenched in an ice bath. The remaining nitrate was measured using a Dionex 2000i ion chromatograph.

RESULTS AND DISCUSSION

In aqueous solution, the sequence (1)-(4) must be altered because reaction (1) would involve mobile ions and is therefore replaced by (1a).



The AM consumption should then become second order, a shift sought in our studies as described next.

The batch kinetics studies were conducted at 350°C on 0.01 M AM solutions, and the progress of the reaction was monitored by following the disappearance of nitrate. The data satisfactorily fit a second-order decay plot, as shown in Figure 10. The rate constant developed from this plot is $3.1 \times 10^{-2} \text{ s}^{-1} \text{ M}^{-1}$.

The first-order rate constant reported by Brower et al. (1989) at 350°C is $3.7 \times 10^{-2} \text{ s}^{-1}$, which corresponds to a half-life ($t_{1/2}$) in the melt of about 19 s. Since for a second-order reaction

$$t_{1/2} = \frac{1}{kA_0}$$

where k is the second-order rate constant and A_0 is the starting concentration of the reactant, we see that the half-life for the solution case at 350°C approaches that for the melt at concentrations of about 1.5 M.

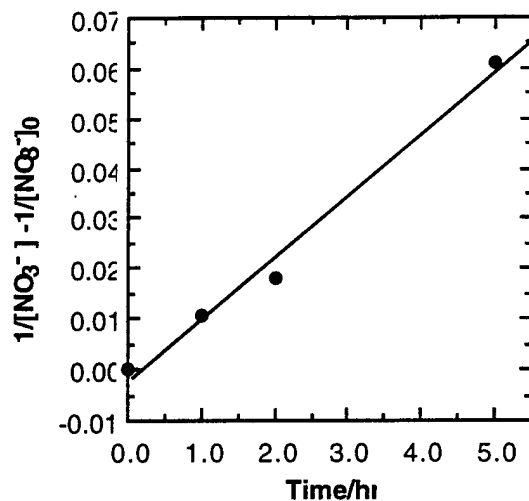


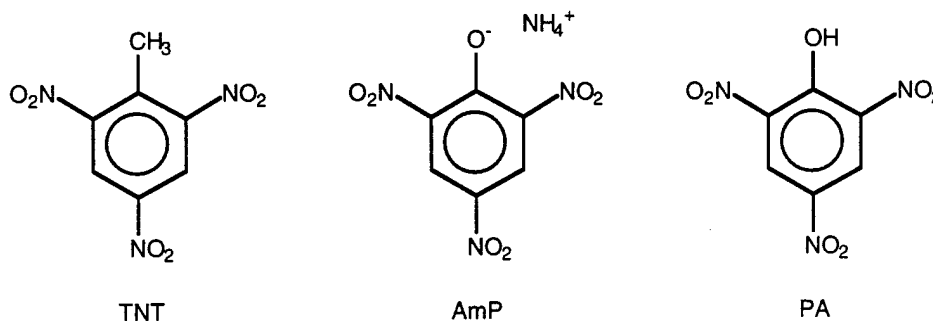
Figure 10. Second-order plot for the loss of nitrate in the hydrothermolysis of ammonium nitrate at 350°C. The starting concentration is 0.01 M.

This is a satisfyingly high value, corresponding to about 12 wt % AN. We interpret this result to suggest that solutions up to 12 wt% as a lower limit can be heated to destroy the AN safely. An extension to AmP suggests that solutions in the range of 32 wt % can be safely heated, a concentration level likely well beyond any loading used in a practical plant situation.

IV. AMMONIUM PICRATE

BACKGROUND

Using a high pressure/temperature spectrophotometer cell for studies in hydrothermal media, we conducted chemical kinetics studies on the decomposition of ammonium picrate (AmP) in liquid water at 260°-320°C. The decomposition products were also studied. AmP is a military explosive, and the effort was conducted to elucidate its chemistry in hydrothermal media as a basis for a technology for its safe disposal. For points of comparison, the hydrothermal decomposition kinetics of the common explosive TNT and picric acid were also examined briefly. The materials share some structural similarities, but the picrates are much more soluble in water. The solubility of TNT



in water at our conditions, however, was sufficient for spectrophotometric monitoring and in all the cases discussed here, the kinetics were obtained for homogeneous systems.

Hydrothermal conditions in this temperature range just below the critical temperature of water ($T_c = 374^\circ\text{C}$) offer an interesting reaction medium. The density is like that of common liquids (Kennedy et al., 1966), but its dielectric constant falls to values of common organic solvents (Lindsay, 1989), and its viscosity falls to values well below the liquid range (Watson, 1980).

Studies of the fate of organic compounds in such hot, subcritical aqueous media have been reported; see, for example, accounts by Townsend et al. (1988) and Lawson and Klein (1985). A large series of reports by Siskin et al. (1993) describe their examination of the behavior of thermally stable cross-links in coal in very hot water. For example, they studied diaryl ethers,

which were shown to undergo acid-catalyzed hydrolyses and were curiously retarded by the addition of some salts.

The use of very hot water as a medium for hazardous waste disposal with no added oxidant can be contrasted to oxidative disposal systems in both subcritical (wet air oxidation) and supercritical water (supercritical water oxidation) in which oxygen is provided. In the present case, since the compounds contain their own internal source of oxidation, no oxidant is added.

We are unaware of any accounts of AmP decomposition or any studies of the exhaustive degradation as reflected in eqs. (1) and (2) for the parent picric acid itself. Kinetics studies of the decomposition of neat picric acid have been reported in the range 183°-270°C (Andreev and Liu, 1963; Kaye, 1978). The process is complex, proceeding in possibly five distinct stages, and an induction period is present to 230°C. At higher temperatures the induction period vanishes. No product data were provided; nor apparently were there any attempts at probing the induction process with added substances.

Some data are available on the thermal degradation of neat TNT, as summarized by Kaye (1978) and Robertson (1948). TNT undergoes autocatalytic decomposition above 150°C, but the rate of reaction approaches characteristic periods of hours only above 200°C. The induction periods fall to seconds above 350°C. The products include some reduced nitrogen in the form of N₂ and N₂O, while some fraction of the organic isolates showed oxidation at the methyl group and oxidative coupling of the arene units. Thus some oxidation/reduction leading to the exhaustive cases in eqs (1) and (2) was seen. The major product of neat pyrolysis, however, is an explosive, nitrogen-containing carbonaceous residue (often referred to as explosive coke), which must result from a complex series of condensation reactions.

EXPERIMENTAL PROCEDURES

Spectrophotometry

The picrate anion offers a convenient chromophore for studying the reaction kinetics spectrophotometrically at about 500 nM. The designs for cell and oven used in geochemical studies (Susak et al., 1981) were adapted for our present use. A sketch of our cell is presented in Figure 11.

The cell body is 316 stainless steel, and the internal volume is about 3 mL. The quartz windows are sealed against the cell body with Rulon/Teflon packing. Temperature of the cell is monitored with a NiCr/NiAl (K-type) thermocouple. The inlet of the cell is connected to an HPLC Pump (WATERS, M-45) through the inlet valve (Whitey, SS-ORS2). The outlet side of

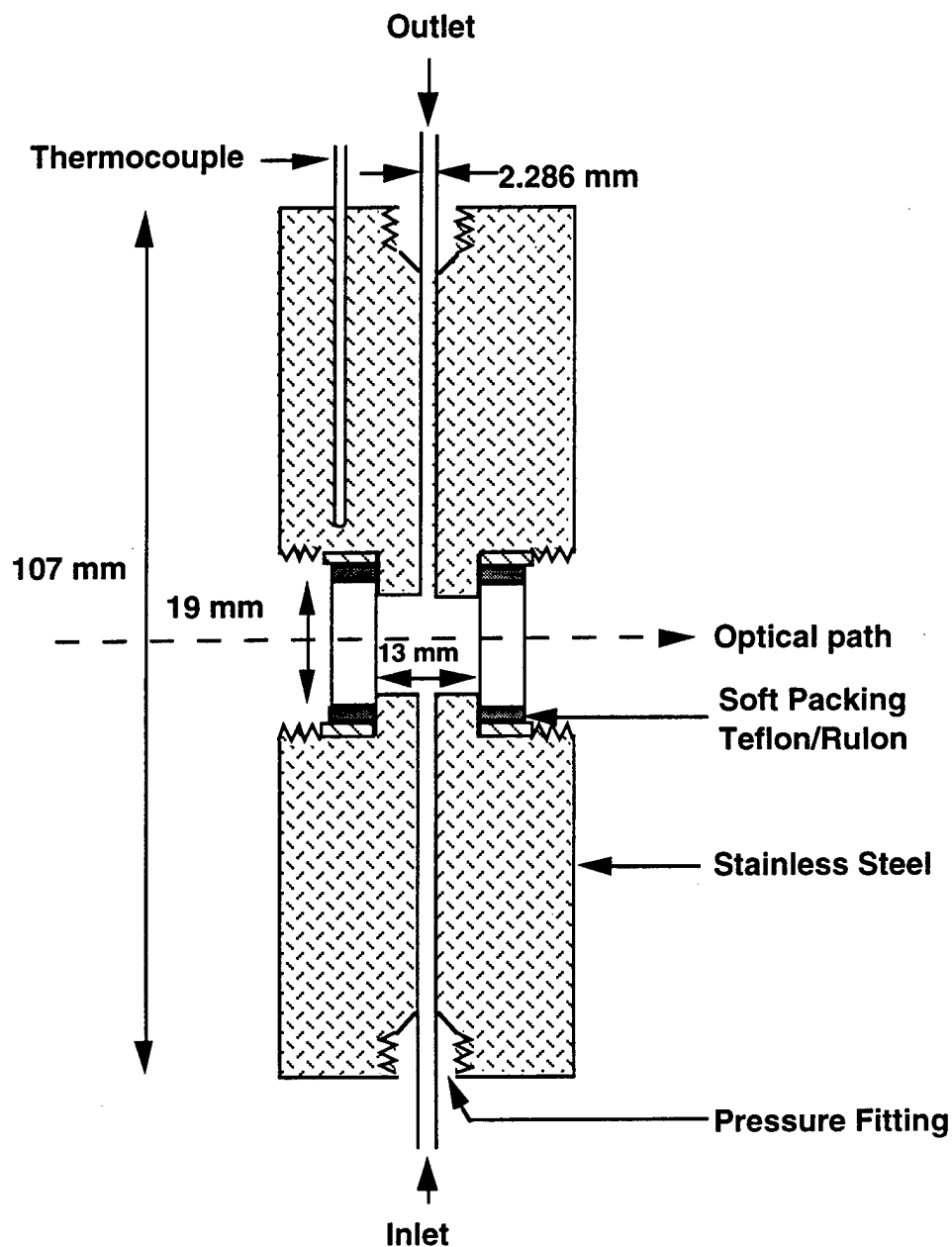


Figure 11. Spectrophotometric cell for kinetics studies in hydrothermal media.

the cell is mated to an Autoclave Engineers high temperature valve (Model No. HT-A13280), which is followed by a NOSHOK pressure gage, a pressure relief valve (Cajon Model No. SS-4R3A, 300-5000 psi), and a shutoff valve (Whitey, SS-ORS2). Throughout the system 1/8-inch SS tubing is used unless specified.

The cell is heated in a snugly fitting resistance tube furnace with circular openings in the optical path. The furnace core is a stainless steel tube wrapped with 5 m of insulated Nichrome wire (0.280 Ω /m). The core is then wrapped with Kaowool insulation and housed within a thin-walled brass tube capped on either end with Transite. To provide thermal protection for the spectrophotometer, the brass housing is then wrapped with a water jacket of soft copper tubing. The entire furnace assembly is mounted on an aluminum plate fashioned to replace the standard sample holder in the spectrophotometer. The temperature is controlled by an Eurotherm temperature controller (808 L1 NO NO QS AKKC 100).

The spectrophotometer itself is a Hewlett Packard Model HP 8452A diode-array instrument interfaced with an HP Vectra VL2 computer operating HP8532 UV-Visible software.

In operation, the system is at room temperature and is flushed with mill-Q water, and a spectrum is obtained to serve as the blank. The oven is then turned on, and when the temperature of the cell reaches the set point, the study solution is pumped through the cell. The pressure of the system is set by adjusting the relief valve. Time required to fill the cell depends on the pumping speed; however, the flow rate should not exceed 1.0 mL/min since the higher flow rates could result in a substantial thermal gradient, which could crack the windows. Once a steady spectrophotometer signal is recorded at the desired wavelength, the run is begun by closing the inlet and outlet valves.

Product Studies

Reactions for product studies used 6.0 mM AmP solutions in 5-mL sealed quartz reactors. The reactors were cleaned initially with acetone and baked at 260°C for a few hours. Once loaded, the reactors were torch sealed under argon. Care was taken not to heat the solution as the vial was being sealed. The reactors were then placed inside stainless steel bombs with enough water present to mimic the head space/liquid volume ratio in the reactor tube, minimizing the pressure stress across the quartz walls.

The bombs were heated in a thermostated oven heated at selected temperatures. Samples were removed at various times and quenched in an ice bath. Remaining picric acid and other organics were determined using a Hewlett Packard 1090 HPLC equipped with a Hypercil C18 column. Inorganic products were determined with a Dionex 2000i ion chromatograph equipped with a conductivity detector. When product gases were determined, the reactions were conducted in stainless steel bombs with quartz inserts.

RESULTS

Kinetic Studies

The first step was to certify the cell operation through comparison with TNT kinetics data obtained in earlier batch studies, and the results of kinetics studies of the hydrothermolysis of TNT in quartz tubes were used (Ross et al., 1993). The comparison of TNT data from both studies at 260°C in Figure 12 shows that the agreement is excellent, as is agreement with a first-order decay which is presented in the figure as the curve for a first-order rate constant of $3.4 \times 10^{-3} \text{ s}^{-1}$. Thus TNT is obviously unstable under these hydrothermal conditions.

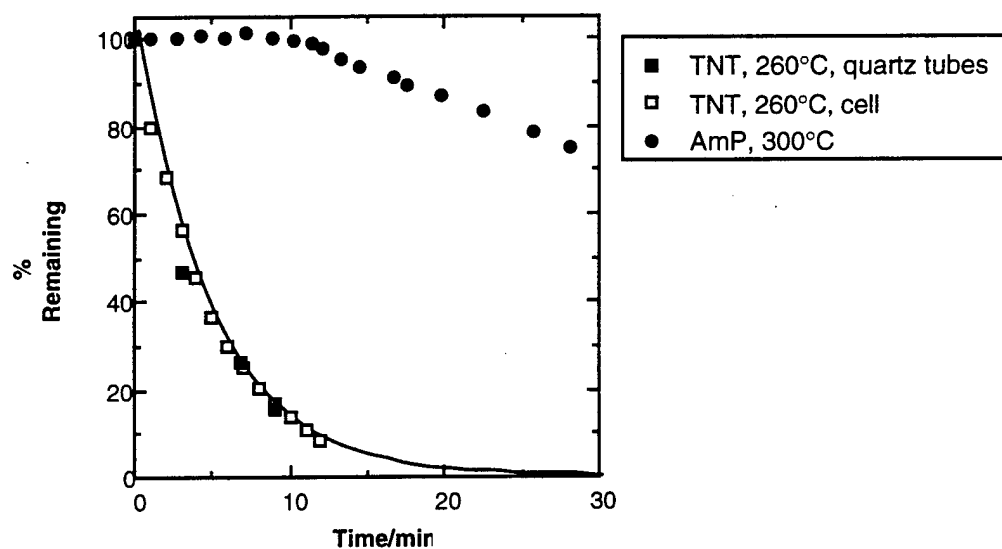


Figure 12. Spectrophotometric monitoring of the decomposition of TNT at 260°C and AmP at 300°C. The curve through the TNT points is that for a first-order decay with a rate constant of $3.4 \times 10^{-3} \text{ s}^{-1}$.

The case for AmP is decidedly different. Figure 12 contains results from our studies with AmP at 300°C for a solution 3.2 mM in AmP and with a starting pH (measured at 25°C) of about 6.7. It is immediately clear from the profile that AmP is considerably more stable than TNT at hydrothermal conditions.* Indeed, AmP is essentially unreactive at these conditions, at least over reasonable periods of time. The question of its practical disposal accordingly becomes a very

* Our earlier TNT work had yielded an Arrhenius expression of $\log k/\text{s}^{-1} = 7.2 - 24/4.6T$, and thus its half-life at 260°C of about 3.5 min falls to 56 s at 300°C (Ross et al., 1993).

major issue, and an understanding of its hydrothermolytic chemistry emerges as a key element in our undertaking.

The profile in Figure 12 includes a prominent induction period, due neither to temperature accommodation nor some other incidental optical effect. Rather, it is a genuine period of minimal reaction, reflecting either accumulation of some reactive material or catalyst or the destruction of an inhibitor. We accordingly conducted a systematic study of AmP, and later picric acid (PA), under hydrothermal conditions, with a focus on the induction period and on the effects of pH and added materials.

AmP was studied over a range of temperatures (280°-325°C) and the induction times varied from about 40 min at the lower temperatures to below 10 min at the highest. The periods of reaction following the induction periods were roughly first order, and an Arrhenius-like plot was prepared based on the half-lives at the various temperatures. Figure 13 shows that satisfactory rates of disposal in such systems will not be easily available.



Figure 13. Plot of half-life vs temperature for the hydrothermolysis of AmP in neutral water.

The effects of pH on hydrothermolysis were studied next, and it is of interest to recall for comparison yet other data from our earlier work with TNT at 200°C (Ross et al., 1993). Figure 14 shows the change in rate as function of the change in starting pH as adjusted by addition of KOH. Over a 4-decade increase in basicity, the rate increase is below a factor of 10. This minor rate effect must be due to secondary effects of the medium; it is clear that the process is not base catalyzed.

Figure 14 also shows the effects of added sodium borate and sodium silicate. Aqueous solutions of these salts are themselves basic, and the data are plotted as a function of those respective pH values. Figure 14 shows a special accelerating effect arising from the addition of

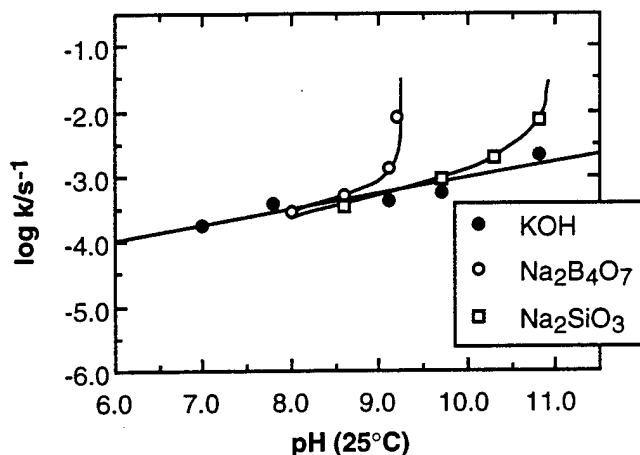


Figure 14. Effects of starting pH on the hydrothermolysis of TNT at 200°C. The pHs are values from measurements at 25°C.

these salts, separate from their basicity. These observations were unexpected since neither borate nor silicate ions possess any obvious feature suggesting catalytic activity. These findings, since extended to a wide range of energetic compounds including nitrate esters and nitramines, were described in a recently issued patent (Ross et al., 1995), and will become important to our delineation of the induction period, as described below.

As for TNT, starting pH had little effect on AmP decomposition rate. This finding is reflected in Figure 15, which presents data from AmP decomposition studies at 300°C and includes for comparison the same profile for AmP shown above in Figure 12. The figure shows that an increase of 5 decades on basicity to 11.9 shortens the induction period somewhat, but does little to the overall rate of destruction. As discussed below, however, the matter is complex and catalysis by base can play some role in the process.

Given our earlier findings that borate and silicate promoted destruction (Ross et al., 1995), we next investigated the addition of borate and silicate. Those results, also presented in Figure 15, show that these additions brought about considerable change. The added salts dramatically eliminated the induction periods, and their profiles are moreover satisfactorily fit by curves calculated for the first-order rate constants noted in the figure caption.

The key finding was provided, next, where PA itself was then studied at pH 12.7. The results presented in Figure 15 show that, at essentially the sample pHs, PA alone and AmP with

silicate decompose at essentially the same rates. Clearly ammonium ion severely slows the decomposition, and silicate and borate in some manner eliminate its retarding effect.

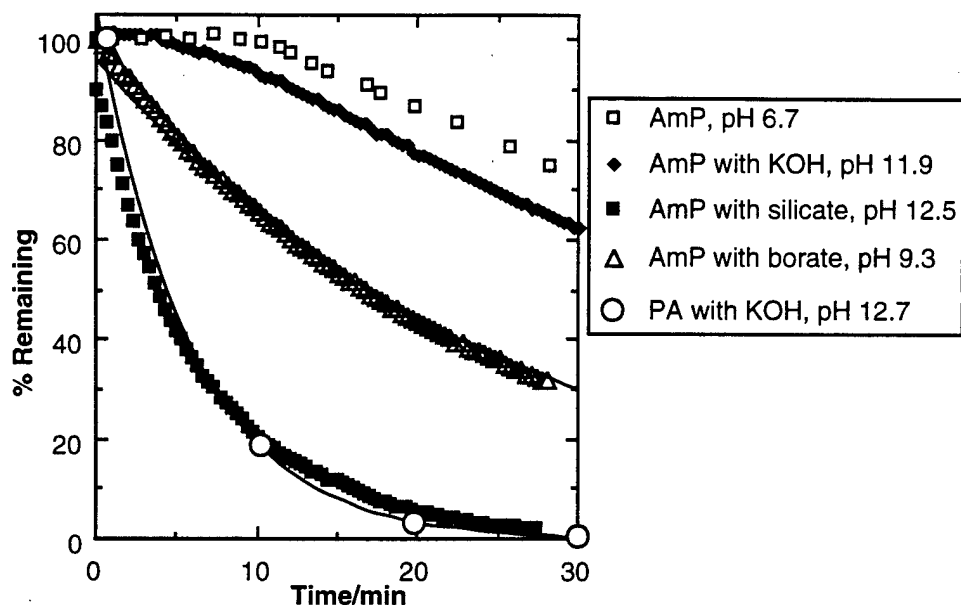


Figure 15. Spectrophotometric monitoring of the decay in the picrate signal at 300°C. The AmP concentration in each case is 3.2 mM. The borate and silicate concentrations, respectively, are 0.025 and 0.050 M. The curves through the borate and silicate points are for first-order decays for rate constants $6.4 \times 10^{-4} \text{ s}^{-1}$ and $2.3 \times 10^{-3} \text{ s}^{-1}$ respectively.

Product Studies

Product studies were conducted for aqueous solutions of AP itself and AP at highly basic conditions at 300°C/30 min. (These conditions represent a period of about 6 half-lives, or 98.5% decomposition.) The results are shown in Table 14.

Table 14 shows satisfactory accounting for both C and N. In the AP-alone case, a considerable fraction of the product was a dark solid that was found to be essentially solely carbon, representing perhaps a quarter of the carbon in the starting AP. Almost 30% of the starting carbon was recovered as acetate, a remarkable conversion considering that the carbon in the acetate methyl group is more reduced than any carbon in the AP. As stated above, acetate is a highly thermodynamically stable species (Latimer, 1952), and its presence in the products reflects the desired thermodynamic control of the process.

As Table 14 shows, the process is moved still further to thermodynamic favor with the addition of base. There are no significant differences in the slate of nitrogen products, but in the

Table 14. Products from the Exhaustive Destruction of PA at 300°C/30 min

Phase	Product	PA alone ^a	PA with 0.1 M KOH ^a
Carbon Gas	CO ₂	31	9
	CO	5	11
	CH ₄	nd	nd
Solution	Acetate	28	60
	Formate	Trace	5
	Glycolate	nd	nd
	Bicarbonate	nd	--
Recovered solid	-	20-30%	<1 ^b
Total C accounted for		85 ⁺	85
Nitrogen Gas ^b	N ₂ O	12	7
	N ₂	39	40
Solution	Nitrite	Trace	3
	Nitrate	Trace	<1
	Ammonium	43	39
Recovered solid	-	<1	<1 ^x
Total N accounted for		94	89

a. Reported as final yields in percent of initial carbon and nitrogen. nd = not detected
b. Very small quantities of a light-colored residue were collected. It was likely silica.

case of carbon, the carbonaceous solid residue is virtually fully eliminated and replaced by additional quantities of acetate.

To understand the hydrothermolytic decomposition more fully, we monitored the formation of nitrite and acetate at 300°C/pH = 12.7, and the results along with the PA profile are shown in Figure 16 (smooth curves are sketched in for convenience). The nitrite is formed at the early stages of the decomposition, then appears to be consumed, coincident with the formation of acetate. This finding is significant and consistent with the fact that only small quantities of nitrite were recovered in exhaustive experiments conducted at 300°C.

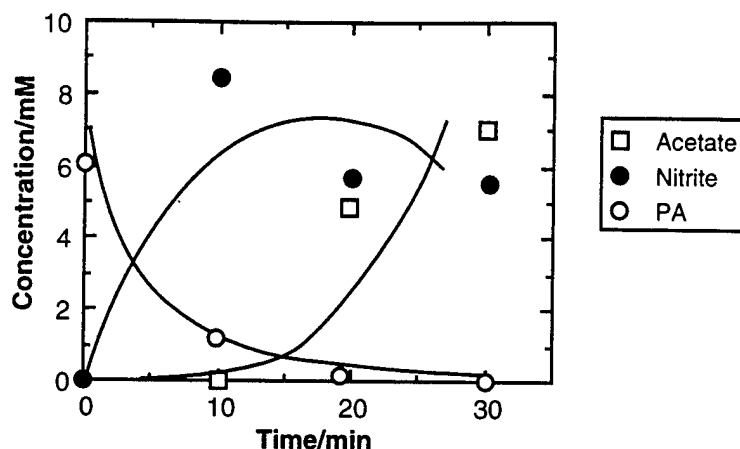
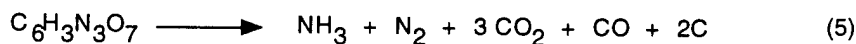


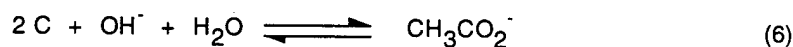
Figure 16. Consumption of PA and formation of nitrite and acetate at 300°C/pH 12.7.

DISCUSSION

The data collected both in the kinetics and product studies reflect a vigorous oxidation-reduction chemistry destroying the picrate anion under hydrothermal conditions. The destruction is complete to simple products, and a stoichiometry reasonably in accord with the data in Table 14 is presented in eq (5).



The equation, however, does not take into account our observation of acetate in the product mixture, and it is of interest to consider the equilibrium in eq (6) which formally depicts the conversion of carbon to acetate.



Although the kinetics of such a process below 600°C must be prohibitively slow, the thermodynamics are surprising. They can be readily examined employing SUPCRT92, a software package for calculating the standard molal thermodynamic properties of minerals, gases, aqueous species, and reactions from 1 to 5000 bars and 0° to 1000°C (Johnson et al., 1992).

The result is presented in Figure 17, which shows that while the conversion to acetate is highly unfavored at lower temperatures, the situation improves with increasing temperature. At temperatures approaching those of our study, the conversion becomes tenable. That favor is undoubtedly reflected in the added-base results in Table 14 in which the carbonaceous residue is essentially fully replaced by acetate. The net result is a stoichiometry like that in eq (7).

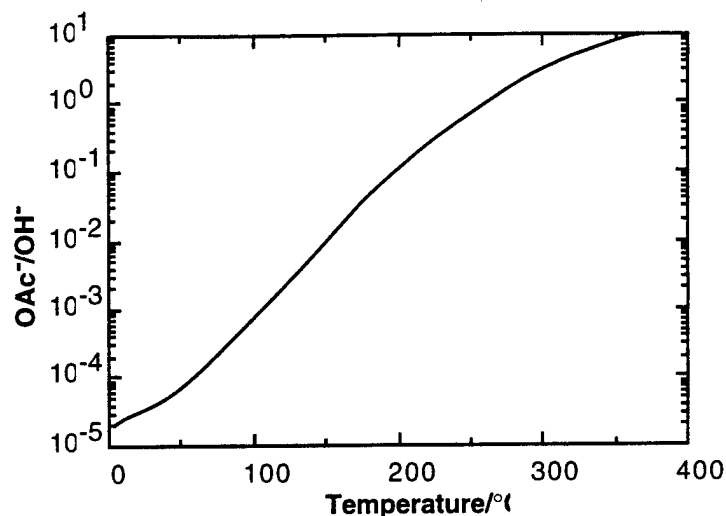
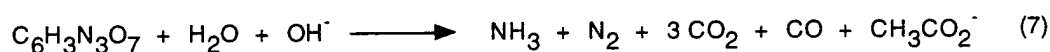
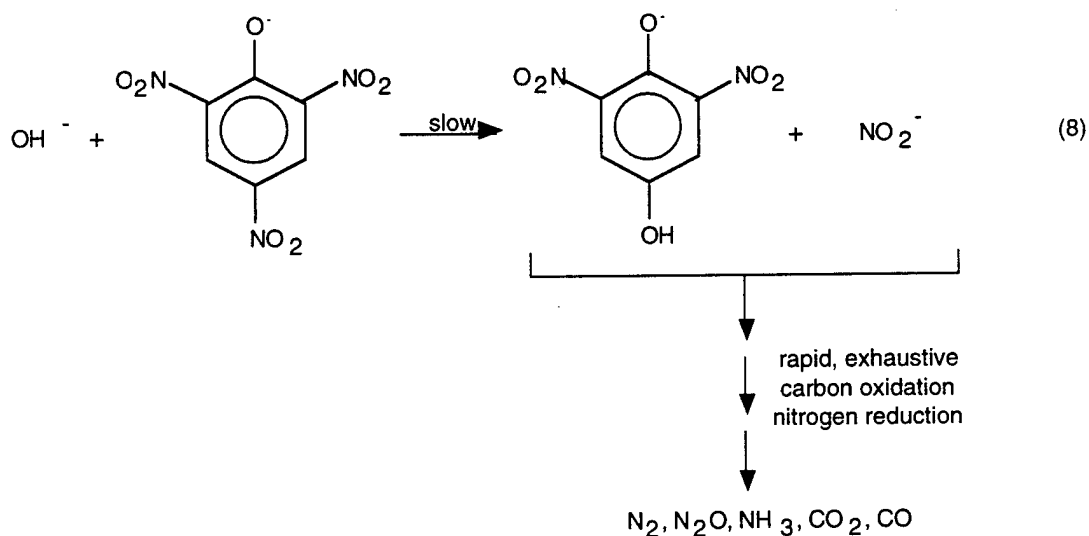


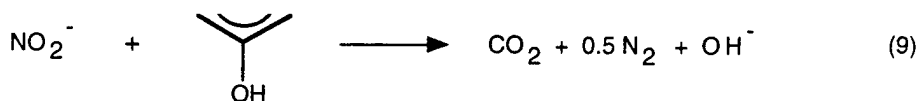
Figure 17. Acetate/OH⁻ ratio as a function of temperature, calculated for eq. (6) along the water liquid-vapor phase boundary to T_c.



The chemical kinetics we have observed for the destruction process are a curious mixture of results, with the ammonium in the AmP apparently severely repressing the rate of destruction, and added silicate and borate salts overriding that action. These results suggest a scheme that is base-catalyzed, starting with the rate controlling displacement of nitrite by OH⁻, as shown in eq (8).

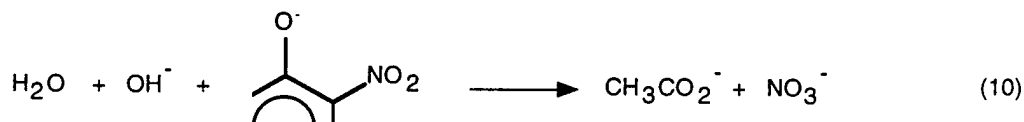


The production of nitrite is key, since nitrite is an active oxidant, while phenols are readily oxidized. Under hydrothermal conditions, oxidation should proceed with ease, while OH^- is regenerated as suggested in eq (9), where nitrite oxidizes a phenolic carbon fully to CO_2 .



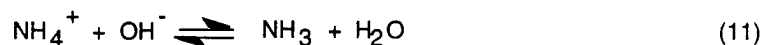
Nitrite production thus triggers a rapid sequence of oxidation, and the full destruction of the arene unit then follows. Under more customary reaction conditions, the suggestion of OH^- attack on the picrate anion in eq (8) might be questioned based on an expected anion-anion repulsion. However, we can expect hydrothermal conditions to bring about reactions not commonly observed at or near ambient temperatures.

Other processes expected are like those in eq (10),



in which the carbons within the arene unit undergo disproportionation and yield acetate. In cases such as these, nitrate is generated, which, like nitrite, is a potent oxidant, and the exhaustive destruction of the starting arene is ensured.

Given the need for base in the sequence as shown by eq (8), we surmise that the intense suppression of picrate hydrothermolysis by ammonium must evolve from the consumption of OH^- by ammonium via eq (11), which under our conditions is driven soundly to the right.



The slow growth of reaction as seen in Figures 12 and 15 would then be expected based on the generation of hydroxide by nitrite action as in eq (9).

To test this premise, we conducted some additional kinetics work with PA in quartz tubes at 260°C at two initial pHs. The results, shown in Figure 18, confirm our postulate. Thus in the strongly basic medium, decomposition proceeds properly in a first-order manner. In the acidic

system, there is no significant reaction initially, but after some time, picrate consumption develops, and the pH of that system increases from the initial 2.4 value to a final value of 7.3, as expected.

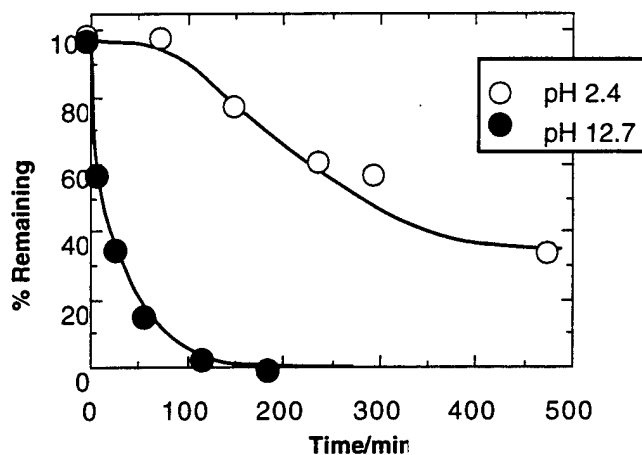


Figure 18. Hydrothermolytic decomposition of PA at 260°C.

The effects added of silicate and borate are thus understood. They are effective because of their polybasic nature and the substantial buffering capacity they can provide. This is a key development in this work because it opens up additional possibilities in meeting the challenge of Explosive D disposal. These possibilities include the use of other inexpensive buffering materials or, in a more process-related vein, available, rugged membrane materials with the proper buffering components attached to the surface.

V. CONCLUSIONS AND RECOMMENDATIONS

A PROPOSED NEW APPROACH

The findings of our program point overall to a safe and rapid conversion of EMs in very hot water to simple, nonenergetic products. Some version of this process can be used satisfactorily as a disposal scheme, followed by a conventional treatment such as biooxidation to convert those products to dischargeable materials. The advantages of such an operation include use of the oxidizing capability of the EMs themselves, thus avoiding the need for added oxygen or other oxidant.

These advantages, however, may not satisfactorily outweigh the need for high throughput and the desire in some cases for complete conversion in a single step. A disposal technology is also needed that would work as well for military wastes not necessarily containing oxidizing groups, such as chemical warfare agents. A broadened hydrothermolysis-based technology can therefore be considered.

Supercritical water oxidation (SCWO) is a major development in hazardous waste disposal, and during our program we began to consider the possibilities of profitably integrating our findings with the needs in SCWO development. In a recent description of that process, Broido pointed out that the prime technology issues still pending in SCWO involve heteroatoms such as chlorine, sulfur, fluorine, and others, which when "present in the material to be treated, . . . form acids during the oxidation process. During the conditions of operations of the supercritical water oxidation reaction these acids can be extremely corrosive" (1996).

Broido explains that added sodium hydroxide neutralizes the acids, but the issue then becomes one of salt handling since the salts, "can build up on the container wall, sometimes to the extent of blocking the flow entirely. A number of solutions to this problem have been tried and are the basis for several proprietary designs, including cycling and flushing, high pressure operations, and others."

A complication in seeking solutions to these problems is a kinetic limitation for some families of feeds, which introduces the need for high temperatures and thus higher pressures. These conditions in turn have restrained the application of new materials and novel composites to the problem, although some very resourceful and inventive applications have been developed.

They include a platinum-lined reactor (General Atomics), diamond-coated reactors (US Navy, US Patent No. 54 616 48), a reactor built as a centrifuge that minimizes corrosion difficulties (US Patent No. 53 727 25), and ceramic-coated reactors (Modar, several patents). None, however, has brought SCWO to the levels of its initial promise advocated by its proponents more than a decade ago.

In summary, the range of wastes SCWO can treat and the degrees to which it can be scaled have limited its development into a robust and commercial-sized operation. Or viewed from a positive perspective, the development of a SCWO modification that both eliminated the acid gas problem while not introducing complex salt handling procedures, and increased oxidation rates, would significantly boost the prospects for the technology. This outlook is the basis of the discussion to follow.

A PROPOSED NEW TECHNOLOGY

Background

The material discussed here includes data developed as part of SRI's Internal R&D program and is proprietary to SRI. A patent application describing the new technology has been filed.

Recognizing the twin goals of eliminating acid gas and salt handling difficulties and accelerating oxidation rates,

A pragmatic look at the development of hazardous waste disposal alternatives to incineration suggests that cooperation between the government and commercial sectors can benefit both sides. Thus the prospect of developing a single, profitable technology that serves both can be key to a sustaining program drawing support from both government and commercial sources.

The needs in the commercial sector are severe. The US chemicals industry, for example, generates 1.5 billion tons of hazardous waste each year. This value compares with the aggregate of 365 million tons of production of the 50 largest volume chemical products, *or a remarkable 4 tons of hazardous waste per ton of product*. A large portion of this discharge is organic, and a suitable means for its treatment remains a major challenge to the technical community.

A portion of that burden that could be both an expedient and timely focus of interest is the 600,000 tons of chlorinated waste each year. This waste is now incinerated at a cost of \$0.20 to \$0.50/lb in certified incinerators that are subject to serious questions of environmental soundness and challenge by environmental groups. A combustion-free technology operating at costs significantly below those values will offer a considerable investment incentive to the private sector. The value of an investment should be enhanced even further by the recent lifting of a ban on PCB imports for disposal. As we will show below, the estimated operating costs for the technology to be described fall as low as \$0.08/lb, well below the incineration costs.

we looked to some of the unexpected phase relationships operating in hot water/salt systems as potential routes to a solution. We concluded that the basis of new technology could reside with the solubility of various salts in liquid water at elevated temperatures, as shown in Figure 19 [developed from data by Keevil (1942) and Morey and Chen, (1956)]. The figure shows the increasing solubility of sodium chloride with increasing temperature, which reflects the behavior of most common salts, including sodium bromide, iodide, nitrate, and most potassium salts. Figure 19 shows, the saturated systems avoid critical behavior.

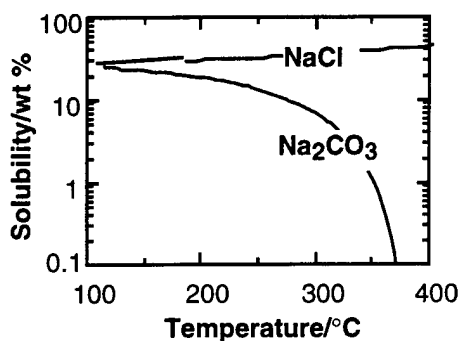


Figure 19. Solubility of sodium chloride and sodium carbonate in liquid water. As noted in the text other salts show these same two classes of behavior.

In contrast, the solubility of sodium carbonate rapidly decreases at higher temperatures. Here critical behavior is observed, with the material becoming fully insoluble at the critical temperature. A few salts behave similarly, including sodium sulfate, sodium fluoride, and sodium phosphate.

Recognizing that sodium carbonate might both eliminate acid gases and accelerate oxidation and that a *heterogeneous* system might promote and advance those activities, we devised a scheme represented by the sketch in Figure 20. In the scheme, an incoming slurry of waste, sodium carbonate, and water is brought to about 380°C/220 atm, or just above the critical point of water. An oxidant such as oxygen (or air) is supplied as shown, and supercritical water oxidation is conducted in what is effectively a fluidized bed of sodium carbonate.

One rationale for the anticipated effectiveness of the system is that the surface activity of the carbonate at these conditions, i.e., suspended in a supercritical water medium at liquid densities at a temperature where its solubility drops to zero, should be substantial. It can be expected to convert chlorine-, nitrogen-, sulfur-, and phosphorus-substituted organic materials readily to the corresponding simple oxygenates. They in turn should then be rapidly oxidized to CO₂ with oxygen. Sodium carbonate is inexpensive and is therefore a suitable consumable.

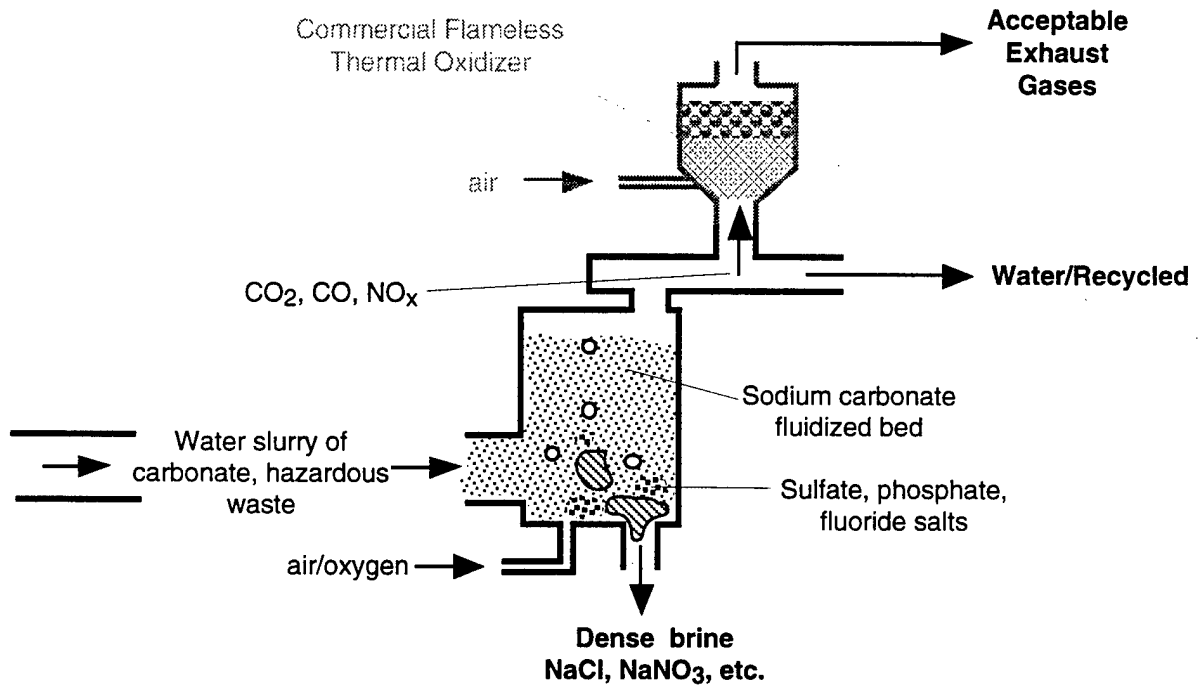
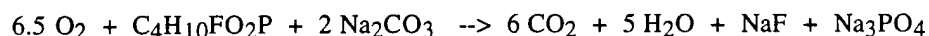


Figure 20. Concept sketch. The process is expected to operate at 380°C/220 atm, or just above the critical point of water. The thermal oxidizer is provisional, to be used in the operation as necessary.

We propose that a large range of wastes can be treated with this technology, including chemical warfare agents, energetic materials, paint sludges, various polymer wastes, and halogenated wastes. The expected stoichiometry for destruction of the chemical warfare agent GB, for example, is



In this case the products NaF and Na₃PO₄ will accumulate over time and join the carbonate as the fluidized bed material. They will remain suspended by the entering fluid medium and not fix at the walls. As discussed below, we have confirmed that at these conditions sodium carbonate accelerates the oxidation, and we expect the product salts to behave in a similar manner. As they accumulate, they can be removed as necessary.*

For the agent HD, the salts would be Na₂SO₄, which would also replace the carbonate over time, and NaCl, which will collect as a dense brine as shown in Figure 20. In all cases we project that the net conversion is the full mineralization of the starting waste atoms. Because the very high ionic strengths of the brines will "salt out" organics to extreme degrees, we are confident that the organic residues in the brines will fall at levels well below detectability.

In the final step the stream can be passed as necessary through a Thermatrix Flameless Oxidizer, which completes the conversion of any trace, nonacceptable volatiles not eliminated in the bed, ensuring an acceptable exhaust stream.

A preliminary process flow diagram for the system is presented in Figure 21. Order of magnitude cost estimates for a 300-gallon per hour (5 gpm) skid-mounted plant operating on a 10 wt% aqueous slurry of waste range from \$2.3 to \$3 million. Operating costs are estimated to be about \$0.45/gallon. For a 300-gpm plant, capital costs are estimated between \$25 million and \$50 million, and the benefits of scale lower the operating costs to \$0.08 per gallon.

Recent Supporting Data

We have conducted a series of internally supported studies in stainless steel batch reactors to confirm our expectation that, under these conditions, the sodium carbonate will scavenge acid gases and its surface will promote oxidation rates. The feeds thus far have been *p*-dichlorobenzene (DCB) and hexachlorobenzene (HCB).

* Recent data in SCWO studies suggest that at least some of the oxidation proceeds at the reactor walls (Savage et al., 1991; Meyer et al., 1995), and we believe that the reactor walls are critical for initiating the oxidation chain reaction. It is thus attractive to consider the purposeful use of the salt surfaces as centers for reaction, effectively replacing metal walls.

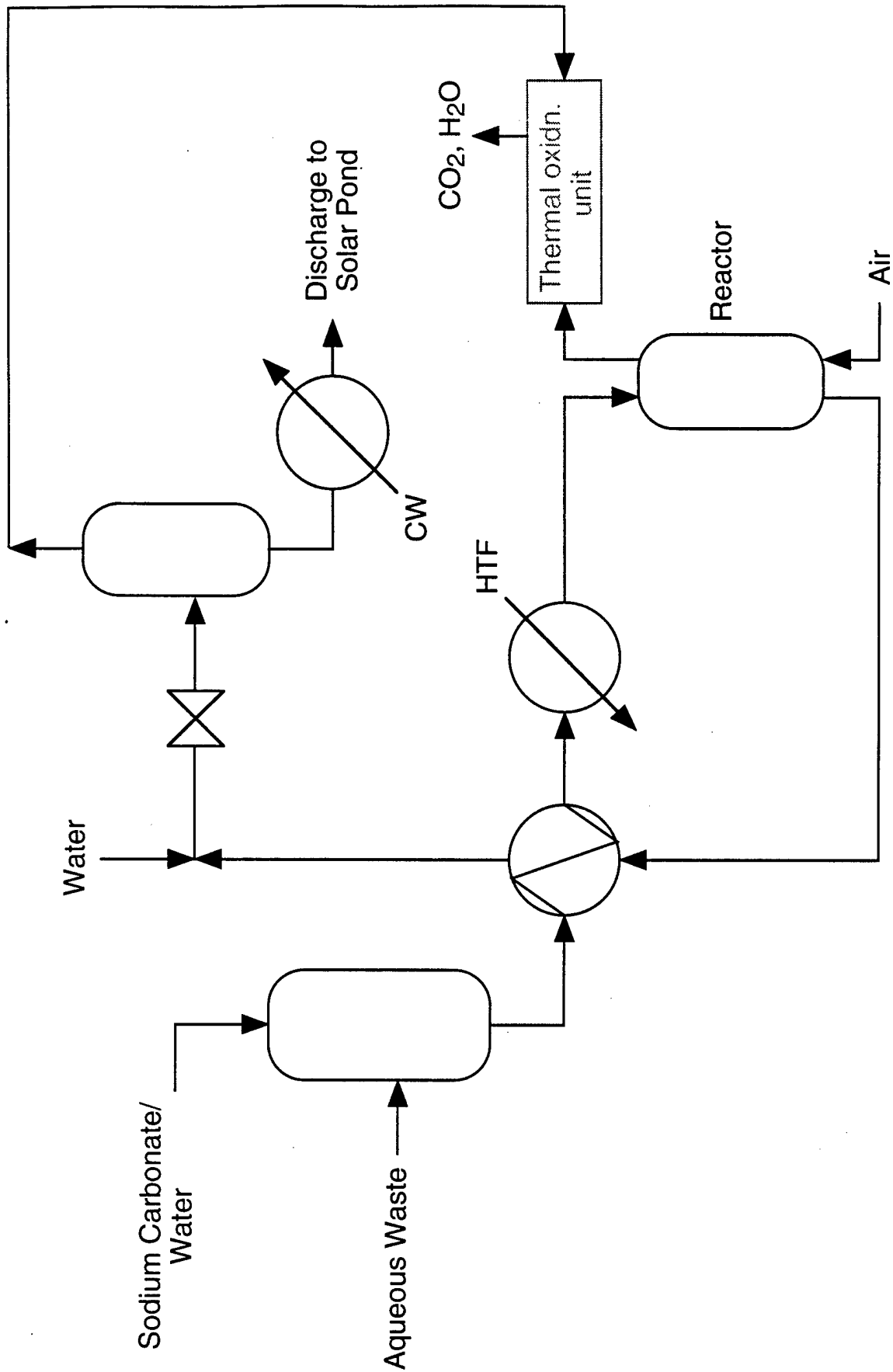
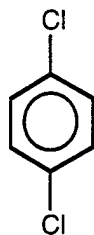
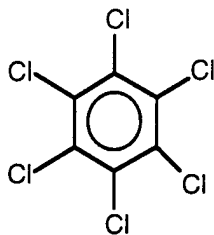


Figure 21. Process flow diagram for carbonate-assisted hydrothermal oxidation. The thermal oxidation unit is provisional, and can be included in the operation as needed.



p-Dichlorobenzene



Hexachlorobenzene

HCB has been used as a fungicide. These compounds both provided abundant quantities of HCl during treatment and, being less reactive than a range of chemical agents, served as agent simulants. Thus a thorough destruction of both DCB and HCB at satisfactory rates would readily reflect conditions adequate for chemical warfare agent treatment.

The DCB studies were conducted at 380°C with 0.12 M DCB and 0.72 M (39 atm) oxygen. The results are presented in Figure 22 and are compared with those reported by Jin et al. (1992) for the conventional SCWO destruction of DCB. The curve labeled SCWO in the figure is derived from their Arrhenius expression, using our conditions and levels of DCB and oxygen. Two attempts in our study to reproduce the Jin et al. data at our DCB levels were unsuccessful due to the high product HCl levels. In both cases previously unused reactors failed during of the runs, and inspection showed the interior surfaces to be very highly corroded. The results of one of the runs is shown in the photograph in Figure 23.

However sodium carbonate-present runs were conducted without incident, and as Figure 22 shows our modification brought about a significant acceleration of the oxidation rate. The isolated product mixture from the 27-min run yielded a total organic carbon (TOC) level of <0.04% of the starting carbon, and thus conversion is essentially complete. Moreover, the interior surface of the reactor, which had been used in several sodium carbonate runs, showed virtually no corrosion due to HCl, as shown in Figure 23.

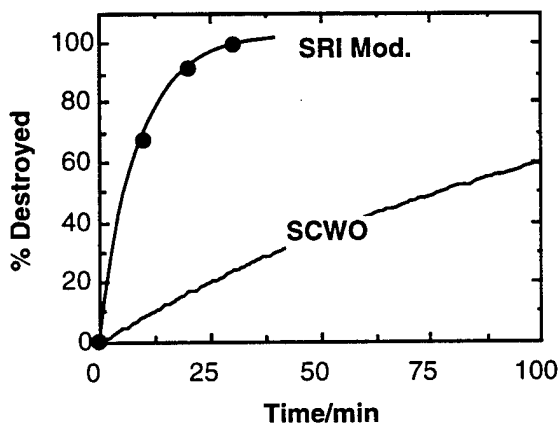


Figure 22. Data from supercritical water oxidation studies on dichlorobenzene at 380°C.

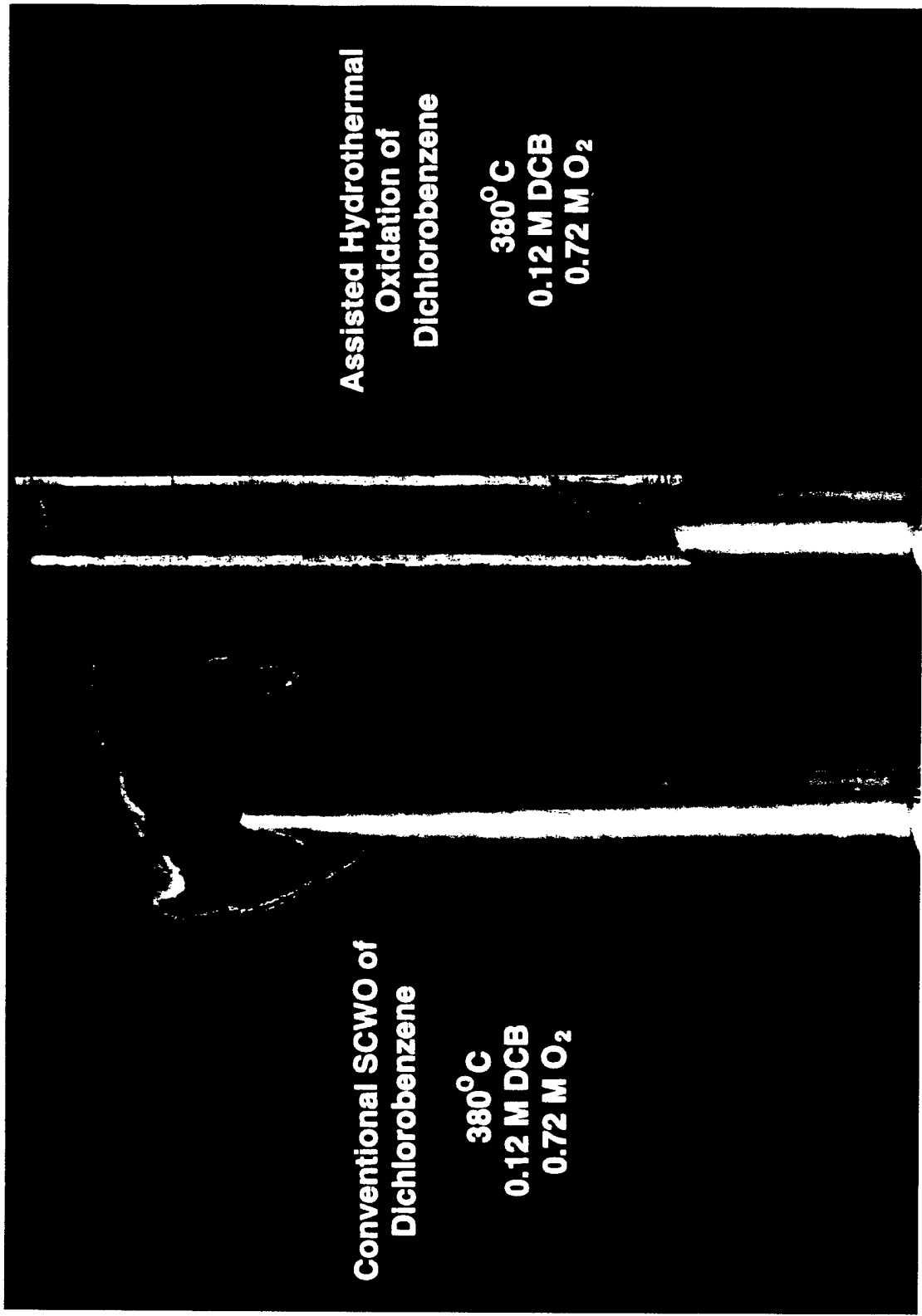


Figure 23. Comparison of interior corrosion and failure of reactor for conventional SCWO of DCB (left) and uncorroded reactor for assisted hydrothermal oxidation of DCB (right).

The studies with HCB were conducted both to confirm the DCB data and to demonstrate the need for water. The data, presented in Figure 24, show that sodium carbonate alone does bring about a slow decomposition. The addition of water, however, clearly results in very rapid HCB destruction.

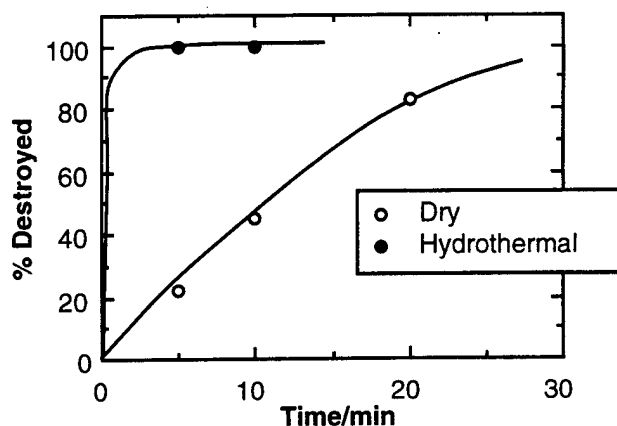


Figure 24. Destruction of hexachlorobenzene at 380°C with sodium carbonate in the presence and absence of water. No oxygen was used in this case. The starting quantities were similar to those used in the DCB work.

SUMMARY AND PROPOSED ACTION

SRI's program for Tyndall AFB has prompted the development of an incineration-free technology concept for the disposal of hazardous military waste. Initial estimates suggest considerable promise for safe, scalable, and economic treatment, as well as profitable utility in the disposal of broader industrial chemical waste.

The present chemical warfare agent incineration is being met with serious public dissatisfaction (for example, Vartabedian, 1996; Ember, 1996), and since the planned incinerators are to be removed after the disposal is complete, even those favoring incineration recognize that many jobs will end with the program.

Given the considerably greater change of acceptance of a disposal process based on hot water, we suggest that the planned chemical weapons incineration be replaced with a technology that could remain after the chemical weapons are disposed of and applied in a profitable, growing enterprise. We thus recommend that some version of the SRI technology be installed in place of an incinerator and used to eliminate the stored agent in the region. The scheme would then call for major portions of the plant to remain in place following completion of the job and the facility transferred to the private sector.

The plant will then be used to destroy chlorinated waste, at least initially, and the profitability of such an enterprise could be significant. If applied to only 10% of the chlorinated waste at costs competitive with conventional incineration, a carbonate-assisted hydrothermal oxidation operation would generate annual revenues of \$20 million. The recent reversal of the ban on importing PCBs for destruction increases the urgency for a sound disposal system and should add significantly to the investment value. The overall net result is timely completion of the weapons disposal task, a satisfied and well employed community, and a healthier environment.

REFERENCES

- Andreev, K. K., and Pao-Feng Liu, 1963. Teoriya Vzryvchatykh Veshchestv, Sb. Satie (1963), 349-63; Chem. Abs., **59**, 13761g (1963).
- Broido, J., 1996. National Defense (28-29 March 1996).
- Brower, K., Oxley, J., and Tewari, M., 1989. J. Phys. Chem., **93**, 4029-4033 (1989).
- Capellos, C., Fisco, W. J., Ribaud, C., Hogan, V. D., Campisi, J., Murphy, F. X., Castorina, T. C. and Rosenblatt, D. H., 1984. *Int. J. Chem. Kinet.*, **16**, 1027-1051 (1984).
- Ember, L., 1996. Chemical and Engineering News, 6 (4 March 1996).
- Jin, L., Ding, Z., and Abraham, M., 1992. "Catalytic Supercritical Water Oxidation of 1,4-Dichlorobenzene," Chem. Eng. Sci., **47**, 2659-2664.
- Johnson, J., Oelkers, E., and Helgeson, H., 1992. Computers and Geosciences, 899-947 (1992).
- Kaye, S., 1978. *Encyclopedia of Explosives and Related Items*, US Army Research and Development Command, Dover, NJ (1978).
- Keevil, N., 1942. "Vapor Pressure of Aqueous Solutions at High Temperatures," J. Am. Chem. Soc., **64**, 841-850.
- Kennedy, G. and Holser, W. 1966. *Handbook of Physical Constants*, Clark, S., Ed. (The Geological Society of America Memoir 97, Section 16, 1966).
- Latimer, W. M., 1952. *The Oxidation States of the Elements and their Potentials in Aqueous Solution* (Prentice-Hall, Inc., New York 1952).
- Lawson, J. and Klein, M., 1985. Ind. Eng. Chem. Fundam., **24**, 203-208 (1985).
- Lindsay, Jr., W. 1989. *The ASME Handbook on Water Technology for Thermal Power Systems*, Cohen, P., Ed., Chapter 7 (The American Society of Mechanical Engineers, 1989).
- Meyer, J., Marrone, P., and Tester, J., 1995. "Acetic Acid Oxidation and Hydrolysis in Supercritical Water," AIChE Journal, **41** 2108-2121.
- Morey, G., and Chen, W., 1956. "Pressure-Temperature Curves in Some Systems Containing Water and a Salt," J. Am. Chem. Soc., **78**, 4249-4252.
- Robertson, A., 1948. Trans. Faraday Soc., **44**, 977-983 (1948).
- Ross, D., Jayaweera, I., Haag, Jr., W., Nguyen, L., and Hum, G., 1993, "Destruction of Energetic Compounds on Soil and in Water by Reductive Hydrothermal Systems," Final SRI Report, Air Force Contract No. 9-X60-G6898-1, 1993.

- Ross, D. S., Jayaweera, I., Nguyen, L., Hum, G., and Haag, W. 1995, "Environmentally Acceptable Waste Disposal by Conversion of Hydrothermally Labile Compounds," US Patent No. 5,409,617, issued April 25, 1995.
- Roth, J., 1950. Addendum to Bull. 6th Army-Navy Solid Propellant Group Meeting, 41 (1950).
- Savage, P., Thornton, T., and Ladue, D., 1991. "Phenol Oxidation in Supercritical Water: Formation of Dibenzofuran, Dibenzo-p-Dioxin, and Related Compounds."
- Siskin, M, Katritzsky, A., and Balasubramanian, M., 1993, Fuel, **72**, 1435-1444 (1993).
- Susak, N. J., Crerar, D. A., Forseman, T. C., and J.L.H. Hass, Jr., 1981, J., Rev. Sci. Instrum. **52**(3), 428-431 (1981).
- Todheide, K., 1982. Ber. Bunsenges. Phys. Chem., **86**, 1005-1016 (1982).
- Townsend, S., Abraham, M., Huppert, G., Klein, M., and Paspek, S., 1988. Ind. Eng. Chem. Res., **27**, 143-149 (1988).
- Vartabedian, R., 1996. Los Angeles Times, A-1 (4 March, 1996).
- Watson, J., 1980, J. Phys. Chem., **9**, 1255-1291 (1980).